number

Report number 25 MDC A6792

Definition of Acceptable Levels of Mismatch for Equivalent Systems of Augmented CTOL Aircraft

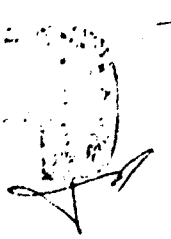

MCDONNELL DOUGLAS

Copy number

Report number 25 MDC A6792

Definition of Acceptable Levels of Mismatch for Equivalent Systems of Augmented CTOL Aircraft

Revision date

Revision letter

Issue date 19 December 1980 Contract number

Prepared by

J. R. Wood
Engineer-Technology
Aerodynamics

J. Hodgkinson
J. Hodgkinson
Unit Chief-Technology
Aerodynamics

Approved by

R. F. Jenny
Branch Chief-Technology
Aerodynamics

In Concurrence

J. F. Mello
Chief Technology Engineer
Aerodynamics

MCDONNELL AIRCRAFT COMPANY

Box 516, Saint Louis, Missouri 63166 – Tel. (314)232-0232

MCDONNELL DOUGLAS CORPORATION

TABLE OF CONTENTS

LIST OF PAGES

Title Page
ii through viii
1 through 22
A-1 through A-26
B-1 through B-5
C-1 through C-5
D-1 through D-5

LIST OF ILLUSTRATIONS

Figure

Table

LIST OF SYMBOLS AND ABBREVIATIONS

CTOL	Conventional Take-Off and Landing
FCS	Flight Control System
F_s	Longitudinal stick force, positive aft, pounds
K_{FS}	Gain in numerator term of longitudinal stick deflection to longitudinal stick force transfer function
$K_{\dot{\theta}}$	Gain in numerator term of pitch rate to longitudinal stick force bare airframe transfer function
L_α	Dimensional lift curve slope, sec^{-1}
MUAD	Maximum Unnoticeable Added Dynamics
n/α	Change of normal load factor with respect to change in angle of attack, g/rad
PR	Pilot rating, Cooper-Harper scale
S	Laplace operator
T_{θ_1}	Phugoid numerator time constant, sec
T_{θ_2}	Numerator time constant in pitch rate transfer function; approximately $1/L_\alpha$, sec
V_{ind}	Indicated velocity, knots
VESA	V/STOL Equivalent Systems Analysis
δ_e	Aircraft elevator deflection, positive trailing edge down, rad
δ_s	Longitudinal stick deflection, positive aft, inches
δ_{FCS}	Damping ratio of Flight Control System actuator
δ_{FS}	Feel System damping ratio
δ_P	Phugoid damping ratio
δ_{SP}	Short period damping ratio
δ_3, δ_4	Damping ratios of control system elements
θ	Pitch attitude, deg
$\dot{\theta}$	Pitch rate, deg/sec

LIST OF SYMBOLS AND ABBREVIATIONS (Continued)

τ_1, τ_2	Lead or lag time constants used in control system dynamics, sec^{-1}
ω_{FCS}	Undamped natural frequency of Flight Control System actuator, rad/sec
ω_{FS}	Feel System undamped natural frequency, rad/sec
ω_P	Phugoid undamped natural frequency, rad/sec
ω_{SP}	Undamped natural short period frequency, rad/sec
ω_3, ω_4	Undamped natural frequencies of control system elements, rad/sec

Subscripts

FCS	Flight Control System actuator
FS	Feel System
P	Phugoid
s	Longitudinal stick
SP	Short Period

ABSTRACT

High order pitch rate frequency responses of augmented aircraft can be broken down into the response of a low order equivalent system, and the mismatch between the response of the actual high order system and the low order equivalent. This study used variable stability NT-33 in-flight data to define frequency response envelopes of acceptable levels of mismatch. The envelopes were narrowest in a region believed to coincide with the piloted crossover region. The computer program for obtaining the equivalent system was then modified to weight the match in the crossover region. Equivalent system summaries for the LAHOS and Neal-Smith data sets are included.

1. INTRODUCTION

Modern flight control systems commonly possess high order responses. Flying qualities analysis using the requirements of MIL-F-8785B (Reference 1), which was written in terms of low order classical aircraft dynamics, is difficult. One proposed method of flying qualities analysis is to match the high order responses with low order equivalent systems, which include an equivalent time delay. The equivalent system parameters are then used for assessment of the overall flying qualities, as described in MIL-F-8785C (Reference 2).

A major difficulty with equivalent systems is that acceptable levels of mismatch between a high order system and its low order equivalent have not yet been defined. The mismatch has been defined by MCAIR as a weighted least squares difference between the gain (and phase) of the high and low order systems (Figure 1).

A recent in-flight simulation using the USAF/Calspan variable stability NT-33, sponsored by both the U.S. Navy and Air Force, examined the flying qualities of high order systems and their low order equivalents. A major objective of this experiment, the Equivalent System Program (ESP), was to define the acceptable levels of mismatch.

Mismatch values of a hundred or so proved unnoticeable to the pilots in the ESP, although previous work (References 3-6) used a mismatch of 10 as an arbitrary criterion of an acceptable fit. The criterion of 10 was based on the visual appearance of the match when observed on a Bode plot; and although it was rooted in instinct rather than science, gave reasonably good results. The insensitivity of pilots to large mismatches in the ESP requires an explanation.

This report offers a theory to explain this insensitivity. The theory agrees with two fundamental principles of manual control theory. Following a brief review of these two fundamentals, they are applied to earlier longitudinal NT-33 data on high order flying qualities. Next the concepts of Unnoticeable and Maximum Unnoticeable Added Dynamics are developed. Finally,

mismatch weighting factors which ensure quality matches are calculated from envelopes of Maximum Unnoticeable Added Dynamics.

2. TWO FUNDAMENTALS OF MANUAL CONTROL THEORY

Studies such as Reference 7 described the human preference for controlled elements with an attitude or attitude rate output which is directly proportional to the input command. The longitudinal short period response of an aircraft can be considered roughly an attitude rate system (Figure 2). The damping and frequency limits of MIL-F-8785 (References 1 and 2) can be similarly considered to constrain deviations from the preferred, K/S response. Flight control systems can be considered as, at best, making the response appear more K/S-like (e.g., by improving damping and frequency), and at worst, introducing high order effects which deviate from the K/S response (e.g., by introducing equivalent time delay).

These studies have also defined a crossover region of manual control. This is the frequency range in which a K/S-like response is desired. For a K/S system, it coincides with the unity amplitude (0 dB) crossover on an open loop Bode plot and with the closed loop bandwidth as shown in Figure 3. The crossover region is essentially the pilot's frequency range of interest.

3. CRITICAL ADDED DYNAMICS

Typical high order aircraft dynamics can be represented by some low order or "base" system with various lead, lag, and pre-filter dynamics added. The addition of these high order dynamics is unnoticeable up to a certain point, after which the pilot notices a change in handling qualities, evidenced by a Cooper-Harper pilot rating differing from that of the original low order system. Addition of high order terms can improve a low order configuration, because the combined effect is that of an improved equivalent system. Usually, however, because of the manual control principles outlined in Section 2, the rating degrades.

Earlier NT-33 simulations, the Neal and Smith experiment (Neal-Smith, References 8 and 9) and the Landing Approach High Order System experiment (LAHOS, Reference 6 and 10), evaluated the effects of several types of added dynamics on fighter handling qualities.

Five types of added dynamics (additions) were investigated. They were first order lead-lags, first order lags, second order lag prefilters, a fourth order lag prefilter, and a second order lag prefilter - first order lead-lag combination. A range of addition values was tested within each addition type. For example, in the LAHOS program, first order lag addition time constants (τ_2) .1, .25, .5, and 1.0 were flown. In this present study, the critical case was defined for each type of addition as the last set of added dynamics to produce a high order configuration that shows no degradation from its base system's pilot rating. This follows the approach of the NADC-sponsored V/STOL Equivalent Systems Analysis (VESA, Reference 11).

For example, Figure 4 shows the frequency responses of a low order system (LOS) along with two high order systems (HOS) derived from it by adding different first order lead-lags. The configuration with the higher frequency lead-lag addition, HOS #1, suffers no pilot rating degradation, but the lower frequency lead-lag addition of HOS #2 causes a definite degradation. The additions in HOS #1 and HOS #2 define unnoticeable and noticeable

added dynamics, respectively. In Figure 5 the mismatch from Figure 4 is plotted. (The mismatch is the difference between the LOS and the two HOS configurations). Based on pilot ratings from Figure 4, a HOS with mismatch falling within the HOS #1 mismatch should have the same pilot rating as the low order system. At some mismatch between HOS #1 and HOS #2, a degradation in rating might be expected. HOS #1 is therefore the critical case for the two first order lead-lag additions shown.

The process of finding the critical cases was readily performed in the VESA because the experiment was designed to evaluate progressive degrees of high order contamination added to low order systems at various frequencies. The Neal-Smith and LAHOS programs were not run with this in mind, and therefore some inference was needed when interpreting the data. Appendix A contains details of the Neal-Smith and LAHOS critical cases. The VESA critical cases defined lateral V/STOL envelopes of Maximum Unnoticeable Added Dynamics (Figure 6), and similarly the Neal-Smith and LAHOS critical cases define longitudinal CTOL envelopes (Figure 7). Another critical case, the LAHOS phugoid, was used to provide low frequency added dynamics similar to VESA cases. In Figure 7, the frequency responses of the critical cases are plotted on a common Bode plot to obtain tentative envelopes (gain and phase) of Maximum Unnoticeable Added Dynamics (MUAD).

As in the VESA, the envelopes defined the pilot's frequency range of interest - the narrow region of the mismatch envelopes. In this frequency range (the crossover region described previously), the narrowing of the envelopes showed that pilots notice much lower values of mismatch than at other frequencies, as would be expected. Section 4 describes the envelopes in detail, and Section 5 explains the transfer function matches to the envelopes.

4. ENVELOPES OF MAXIMUM UNNOTICEABLE ADDED DYNAMICS

The Neal-Smith and LAHOS critical added dynamics were found and then drawn on a common Bode plot as described in the previous section and Appendix A. However, the critical added dynamics were all at high frequencies (i.e., at or above the crossover frequency) unlike the VESA critical dynamics, which included both high and low frequency additions. Examination of the VESA envelopes, which were wider at low frequencies than at high ones, suggests that a pilot will tolerate relatively large gain or phase mismatches at low frequencies. However a rational method of establishing the CTOL envelopes at low frequencies was needed. The LAHOS or NT-33 phugoid was the sole contamination of the K/S shape in this region, and did not evoke adverse pilot comments. The phugoid low frequency transfer function is:

$$\left.\frac{\dot{\theta}}{F_s}\right|_{\text{phugoid}} \simeq \frac{S(S + 1/T_{\theta_1})}{S^2 + 2\zeta_p\omega_p S + \omega_p^2}$$

$$T_{\theta_1} = 11.77$$
$$\zeta_p = .135$$
$$\omega_p = .196$$

This phugoid, the basic shape of the VESA envelopes, and considerable engineering judgement were used to shape the low frequency portion of the gain and phase envelopes. The phugoid requirements of MIL-F-8785C (Reference 2) offered no guidance as the phugoid frequency was not specified.

The envelopes were drawn by fairing smooth curves either through or tangent to parts of the various added dynamics. The four envelope curves (an upper and a lower for gain and phase) were tabulated as a function of the frequency and then matched by transfer functions using an interactive matching program (see Appendix B). The resulting transfer functions define the envelope boundaries, are more compact than tables, and can be used for any frequencies and frequency ranges within the limits of 0.1 and 100 rad/sec. These transfer functions are:

Upper Gain Envelope:

$$\frac{3.16S^2 + 31.61S + 22.79}{S^2 + 27.14 + 1.84}$$

Lower Gain Envelope:

$$\frac{9.55E\text{-}2S^2 + 9.92S + 2.15}{S^2 + 11.60S + 4.95}$$

Upper Phase Envelope:

$$\frac{68.89S^2 + 1100.12S - 275.22}{S^2 + 39.94S + 9.99} e^{.0059S}$$

Lower Phase Envelope:

$$\frac{475.32S^2 + 184100.S + 29456.1}{S^2 + 11.66S + 3.89E\text{-}2} e^{-.0072S}$$

These transfer functions provide good approximations to the tentative envelopes of Maximum Unnoticeable Added Dynamics as shown in Figure 8, and can be used to examine the quality of matches between high order systems and their equivalents. A mismatch falling within the envelopes indicates that the associated low order equivalent system is satisfactory as a flying qualities tool. The envelope transfer functions can also be used as a design tool to predict whether a set of added dynamics will be noticed by a pilot.

5. MISMATCH WEIGHTING

The mismatch envelopes allow determination of equivalent system match quality, whatever match method has been used. Since the envelopes imply that a close match is needed in the crossover region, it makes sense to try to ensure this close match by some means. Two possible methods of doing this are:

1) Penalize the match by adding a large constant to the mismatch function whenever the added dynamics fall outside the envelope; and
2) At any frequency apply a weighting factor which is an inverse function of the allowable mismatch at that frequency.

The penalty method was rejected because of two major faults which would require correction to ensure the desired match quality (see Appendix C). It is therefore simpler to use the second method (weighting factors) to get good matches.

The mismatch weighting factors can now be calculated for any frequency in a chosen range, because the allowable mismatch envelopes are defined as continuous functions. In this study the chosen range was from .1 to 100 rad/sec. The weighting factors are based on the allowable gain and phase mismatch from the Maximum Unnoticeable Added Dynamics envelopes, along with the definition of the mismatch function. Since the mismatch function at any frequency was defined as the square of the difference between the high and low order systems' frequency responses at that frequency, the weighting factors are similarly based on the square of the allowable additions at the frequency, as described in Appendix C.

The mismatch weighting factors calculated from the CTOL gain and phase MUAD envelopes are shown in Figure 9. The weighting factors result from equating the mismatch along the gain and phase envelope curves. The gain weighting factors at a particular frequency were calculated by dividing the largest allowable gain mismatch by the allowable mismatches (upper and lower) at that frequency. The phase weighting factors were calculated similarly. Thus the weighting is largest when the envelopes are narrowest. Because the envelopes are not symmetric about the 0 dB and 0

degree lines, there are separate upper and lower sets of weighting factors. The choice of upper or lower weighting depends on the signs of the gain and phase differences being weighted. With these weighting factors, good crossover region matches can be obtained by sacrificing somewhat the quality of the match outside the crossover region.

6. SUMMARY AND RECOMMENDATIONS

Using variable stability NT-33 in-flight data, it was shown that high order pitch rate frequency responses of augmented aircraft can be broken down into two components:

1) The response of a low order equivalent system (with augmented frequency, damping, and time delay values which can be compared with MIL-F-8785C requirements); and
2) The mismatch, the difference between the responses of the actual high order system and the low order equivalent.

This study defined the acceptable levels of mismatch (2), regardless of the method used to obtain the equivalent system (1). The method of obtaining the equivalent system was then modified to increase the likelihood of meeting the mismatch criteria.

The acceptable levels of mismatch were obtained by defining frequency response (Bode) envelopes of Maximum Unnoticeable Added Dynamics (MUAD). The likelihood of meeting the mismatch criteria was then increased by defining mismatch weighting factors as a function of the MUAD envelopes and therefore of frequency. The envelopes and the weighting factors agree with the two related manual control theory concepts of the desirability of a K/S response and the importance of the crossover region; the envelopes are significantly narrower in the crossover region, and similarly the associated weighting is largest in the crossover region.

The envelopes developed in this study are tentative because the data were not from programs specifically conducted by progressively adding high order dynamics to determine which were unnoticeable and which were not. Some engineering judgement was therefore necessary.

To check or improve the accuracy of the envelopes, the effects of various added dynamics could be investigated in future simulations, either in-flight or fixed base. The simulations could be used to expand or fill in gaps in present configuration matrices. Although the work done involved CTOL longitudinal dynamics, a similar approach to lateral and directional dynamics is warranted. Lateral and directional data for demanding tasks are lacking,

however the longitudinal envelopes agree with general principles of manual control theory and are similar to envelopes developed for lateral hovering dynamics as Figure 10 shows. They are therefore useful as tentative tools for lateral and directional equivalent system determination.

It should be noted that the MUAD envelopes allow for larger mismatches than those normally seen in matching-developed flight control system (FCS) designs. This apparently is the explanation for the Equivalent System Program (ESP) results, in which large mismatches were unnoticeable to pilots. Preliminary results also indicate that the new weighting factors do not alter equivalent system parameters significantly for those configurations which were reasonably matched without the weighting. Further verification of this is required, however.

7. REFERENCES

1. Anon, Military Specification, Flying Qualities of Piloted Airplanes, MIL-F-8785B (ASG), Amended 16 September 1974.
2. Anon, Military Specification, Flying Qualities of Piloted Airplanes, MIL-F-8785C (ASG), February 1980.
3. Hodgkinson, J., LaManna, W. J., and Heyde, J. L., "Handling Qualities of Aircraft with Stability and Control Augmentation Systems - A Fundamental Approach," Journal of the Royal Aeronautical Society, February 1976.
4. Hodgkinson, J., Berger, R. L., and Bear, R. L., "Analysis of High Order Aircraft Flight Control System Dynamics Using an Equivalent System Approach," MCAIR Report 76-009, Seventh Annual Pittsburgh Conference on Modeling and Simulation, 26-27 April 1976.
5. Hodgkinson, J., "Equivalent Systems Approach for Flying Qualities Specification," MCAIR Report 79-017, SAE Aerospace Control and Guidance Systems Committee Meeting, 7-9 March 1979.
6. Johnston, K. A., and Hodgkinson, J., "Flying Qualities Analysis of an In-Flight Simulation of High Order Control System Effects on Fighter Aircraft Approach and Landing," MDC Report A5596, December 1978.
7. McRuer, D. T., and Krendel, E. S., "Mathematical Models of Human Pilot Behavior," AGARDograph No. 188, January 1974.
8. Neal, T. P., and Smith, R. E., "An In-Flight Investigation to Develop Control System Design Criteria for Fighter Airplanes," AFFDL-TR-70-74, December 1970.
9. Boothe, E. M., Chen, R. T. N., and Chalk, C. R., "A Two-Phase Investigation of Longitudinal Flying Qualities for Fighters," AFFDL-TR-74-9, April 1974.
10. Smith, R. E., "Effects of Control System Dynamics on Fighter Approach and Landing Longitudinal Flying Qualities (Vol. I)," AFFDL-TR-78-122, March 1978.
11. Carpenter, C. G., and Hodgkinson, J., "V/STOL Equivalent Systems Analysis," NADC-79141-60, May 1980.

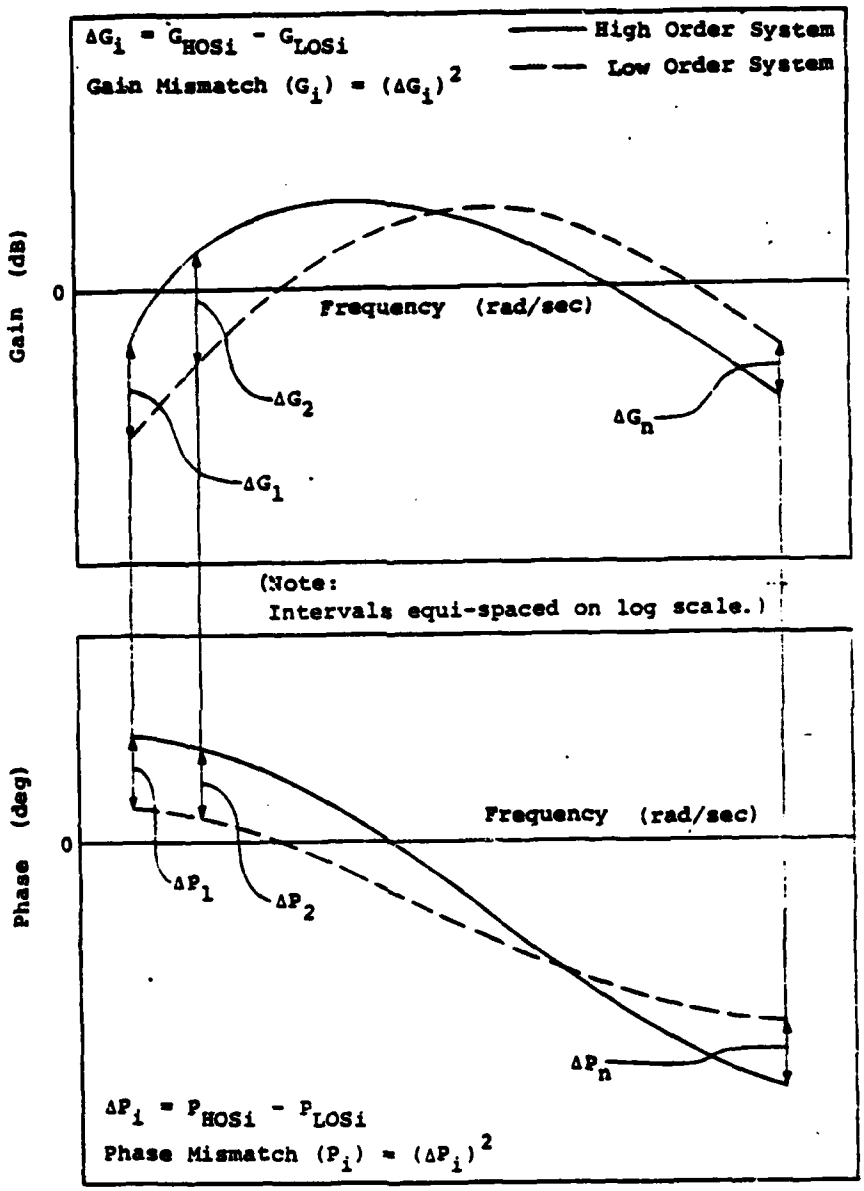

$$\text{Total Mismatch} = \frac{20}{n} \sum_{i=1}^{n} (G_i + .02P_i)$$

FIGURE 1 DEFINITION OF MISMATCH

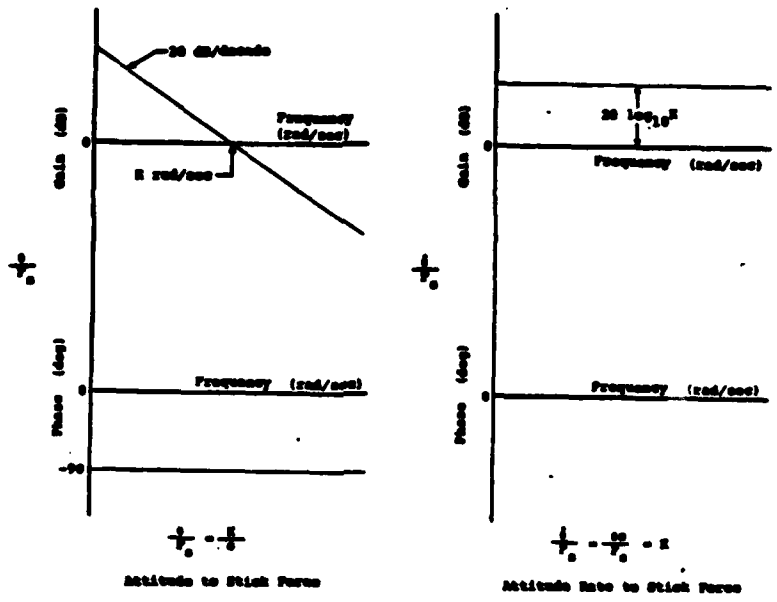

FIGURE 2 ATTITUDE AND ATTITUDE RATE TO STICK FORCE RESPONSES

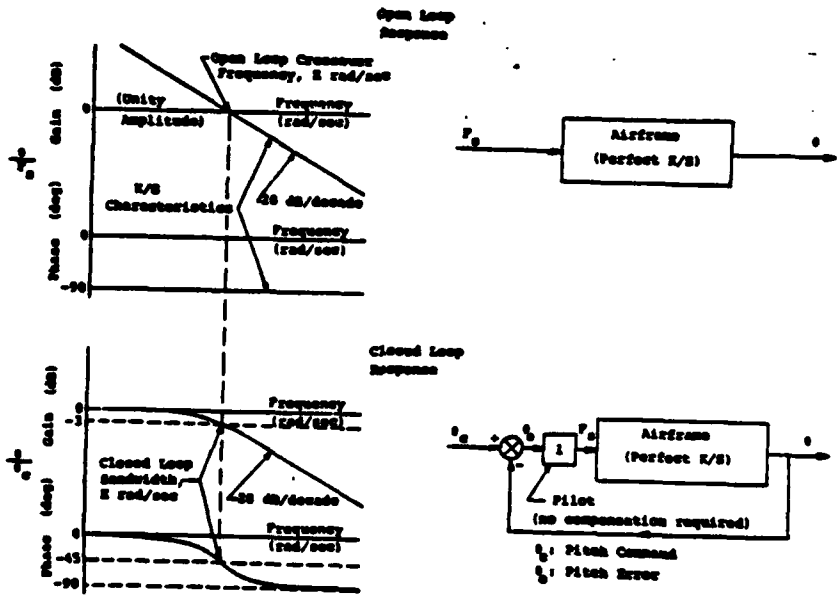

FIGURE 3 DEFINITION OF THE CROSSOVER REGION

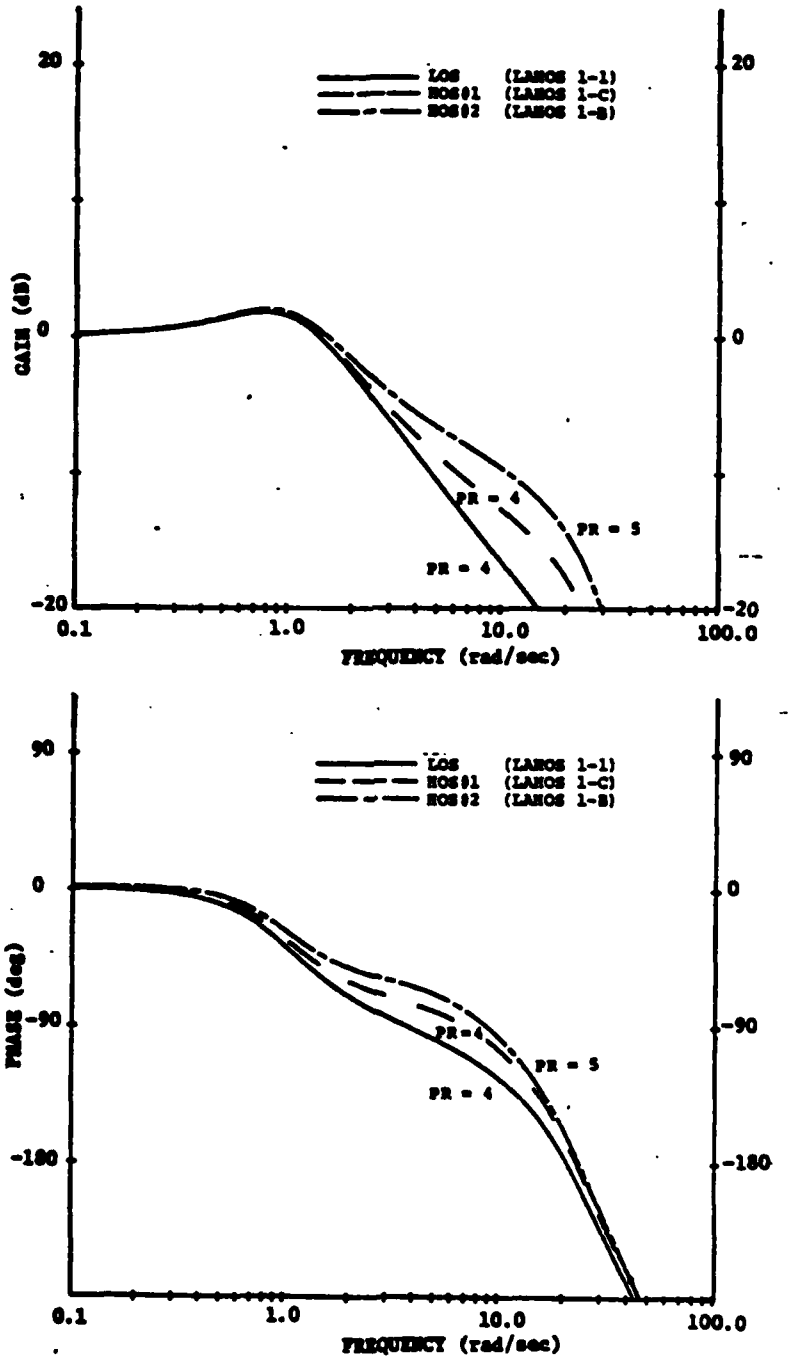

FIGURE 4 ADDITION OF UNNOTICEABLE AND NOTICEABLE DYNAMICS TO A LOW ORDER SYSTEM (EXAMPLE)

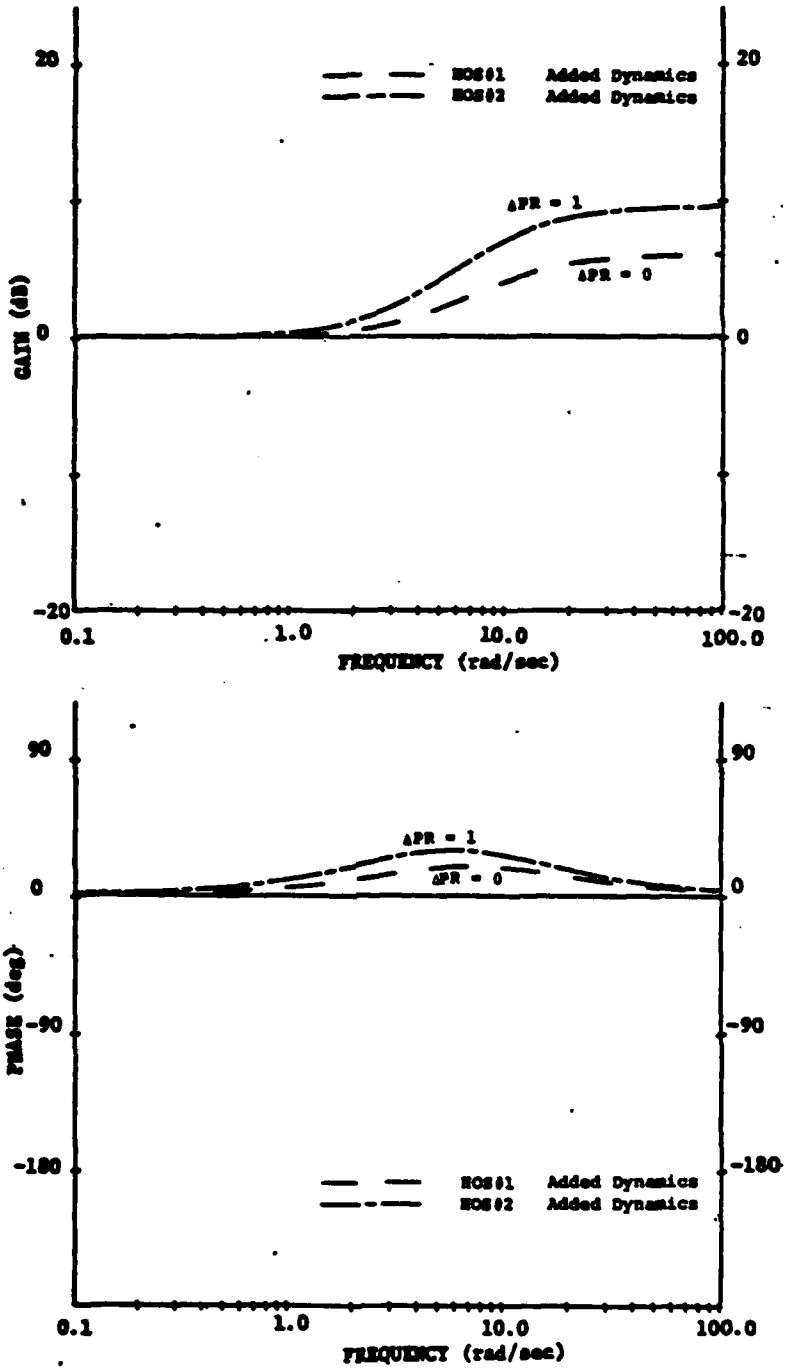

FIGURE 5 MISMATCH FROM UNNOTICEABLE AND NOTICEABLE ADDED DYNAMICS (EXAMPLE)

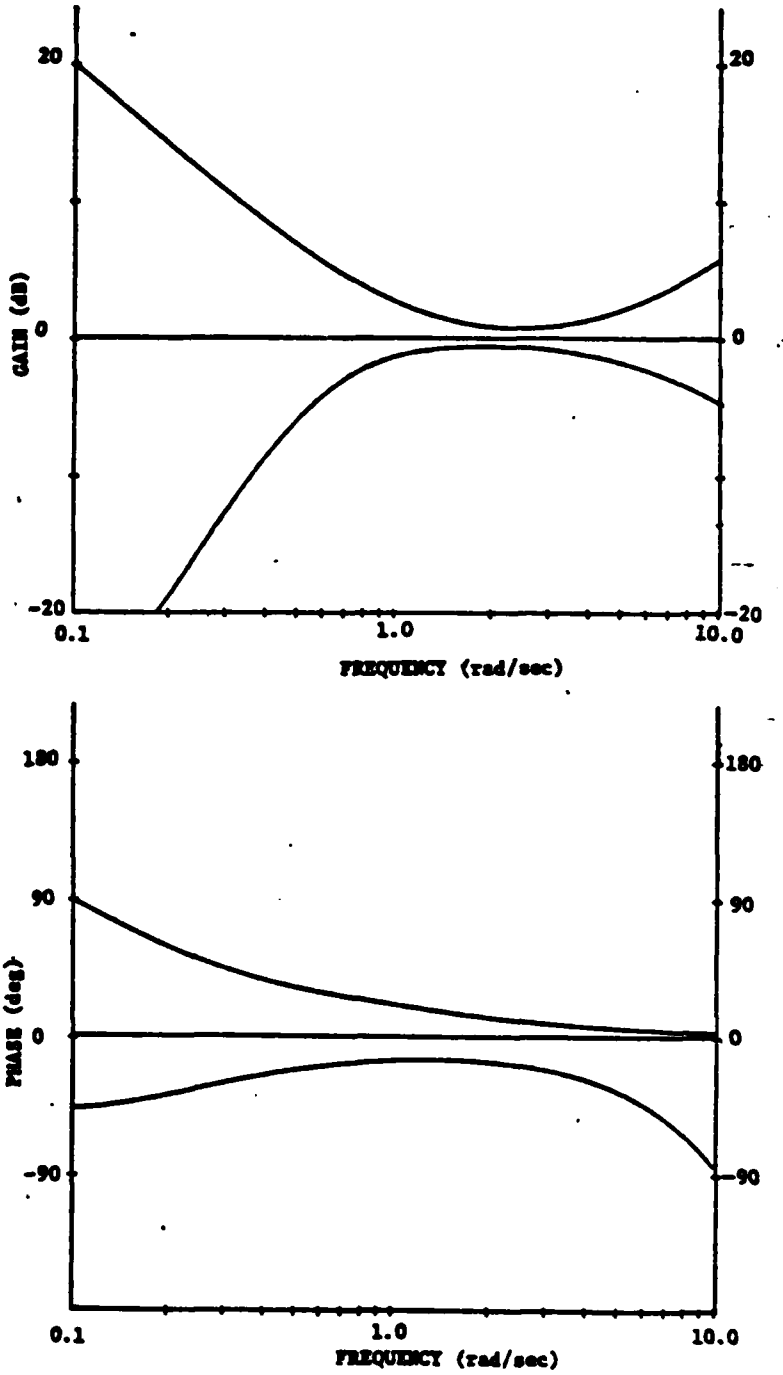

FIGURE 6 VESA ENVELOPES OF MAXIMUM UNNOTICEABLE ADDED DYNAMICS

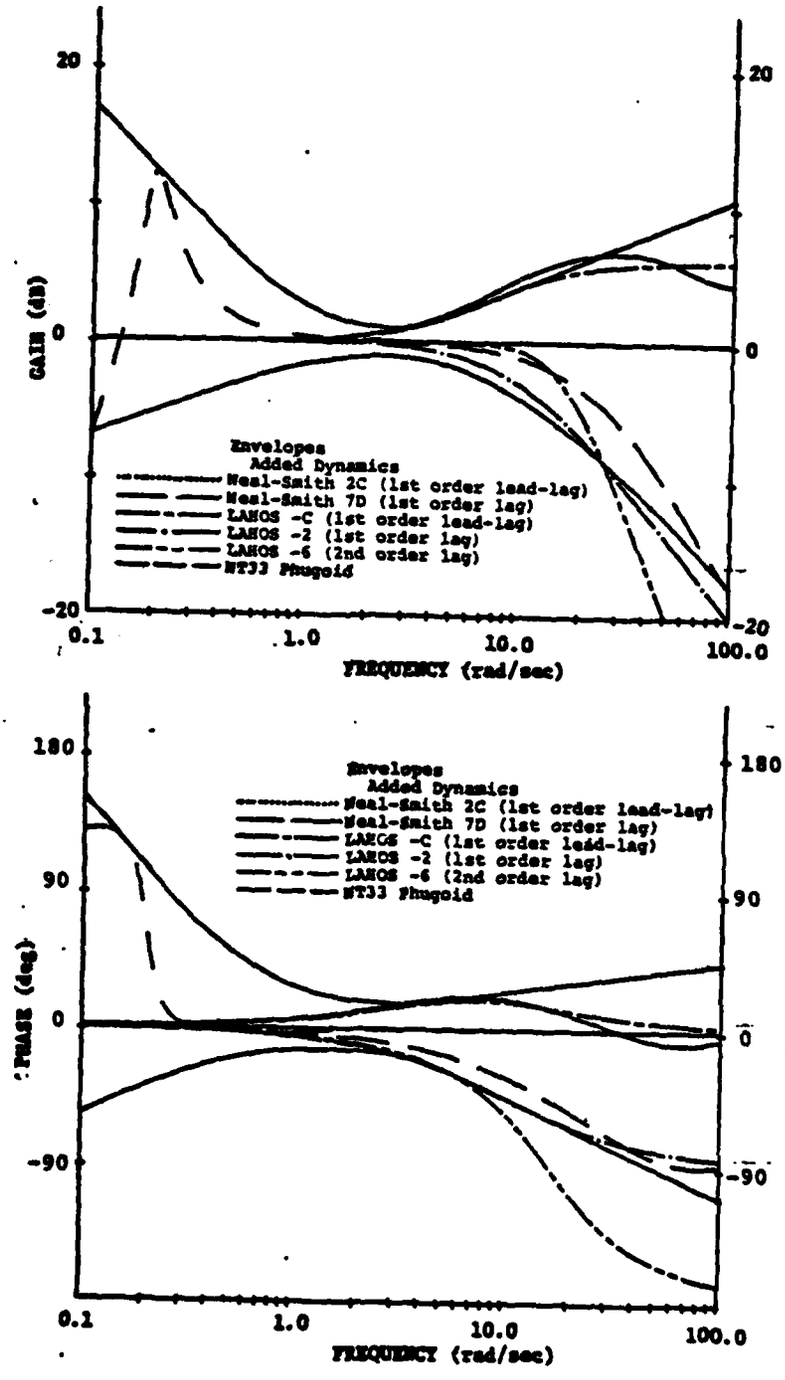

FIGURE 7 CTOL CRITICAL ADDED DYNAMICS AND ENVELOPES

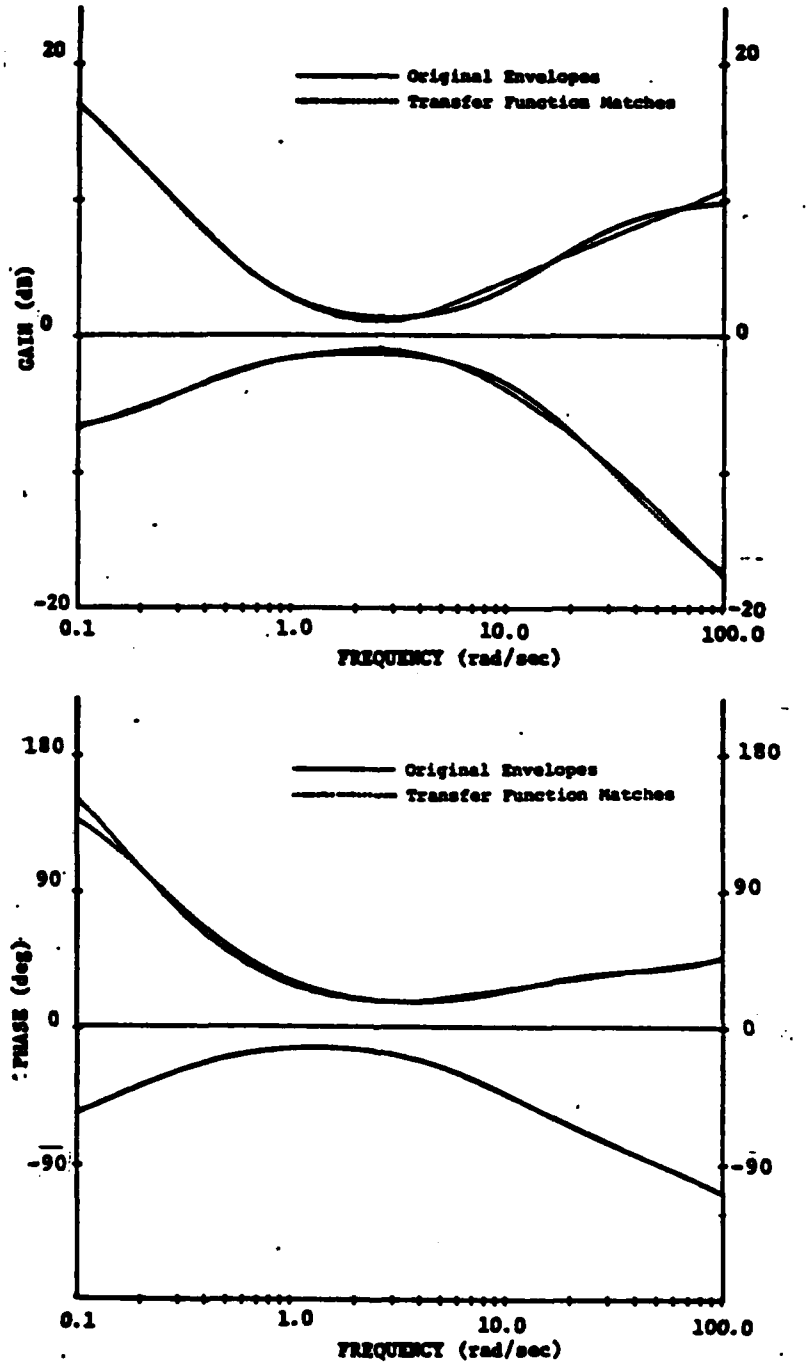

FIGURE 8 CTOL ENVELOPES AND TRANSFER FUNCTION MATCHES

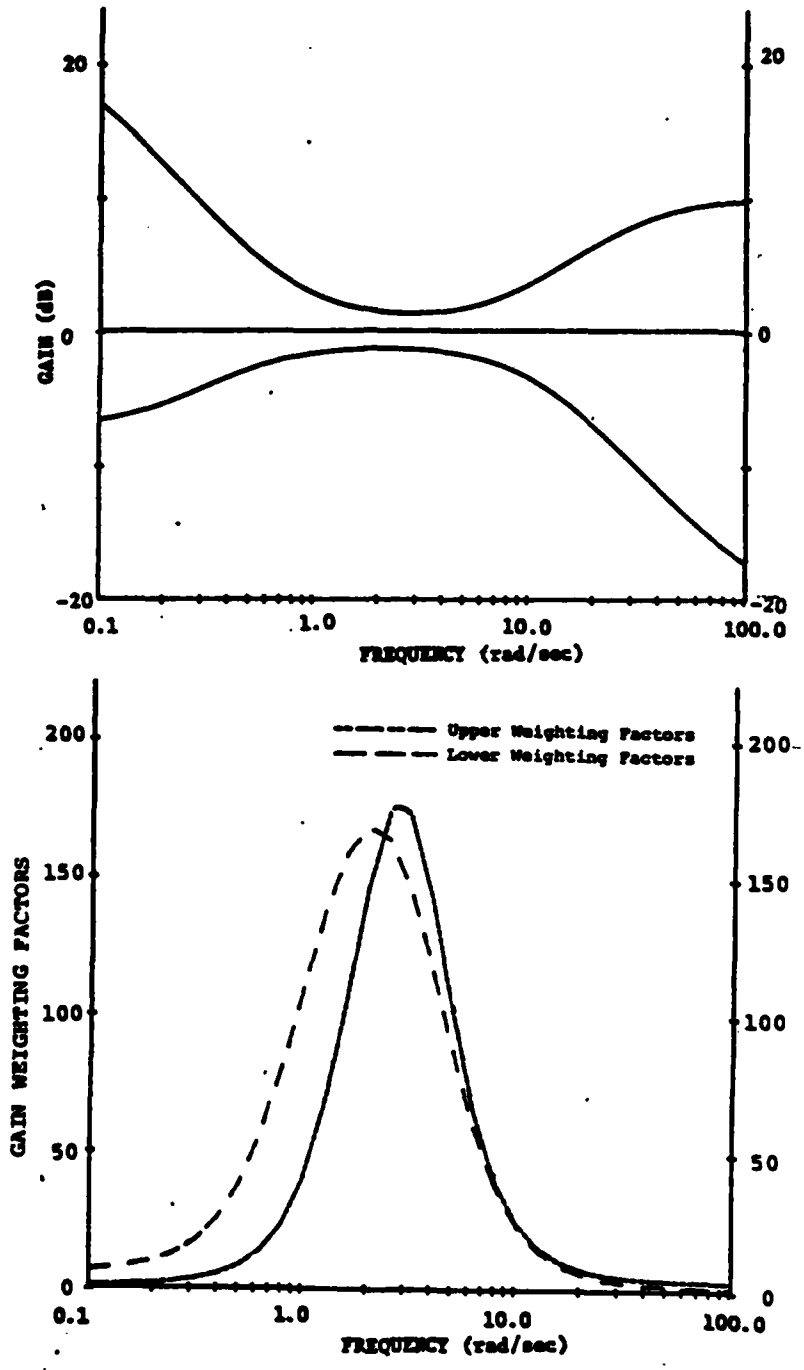

FIGURE 9 CTOL ENVELOPES OF MAXIMUM UNNOTICEABLE ADDED DYNAMICS (TRANSFER FUNCTIONS) AND ASSOCIATED WEIGHTING FACTORS

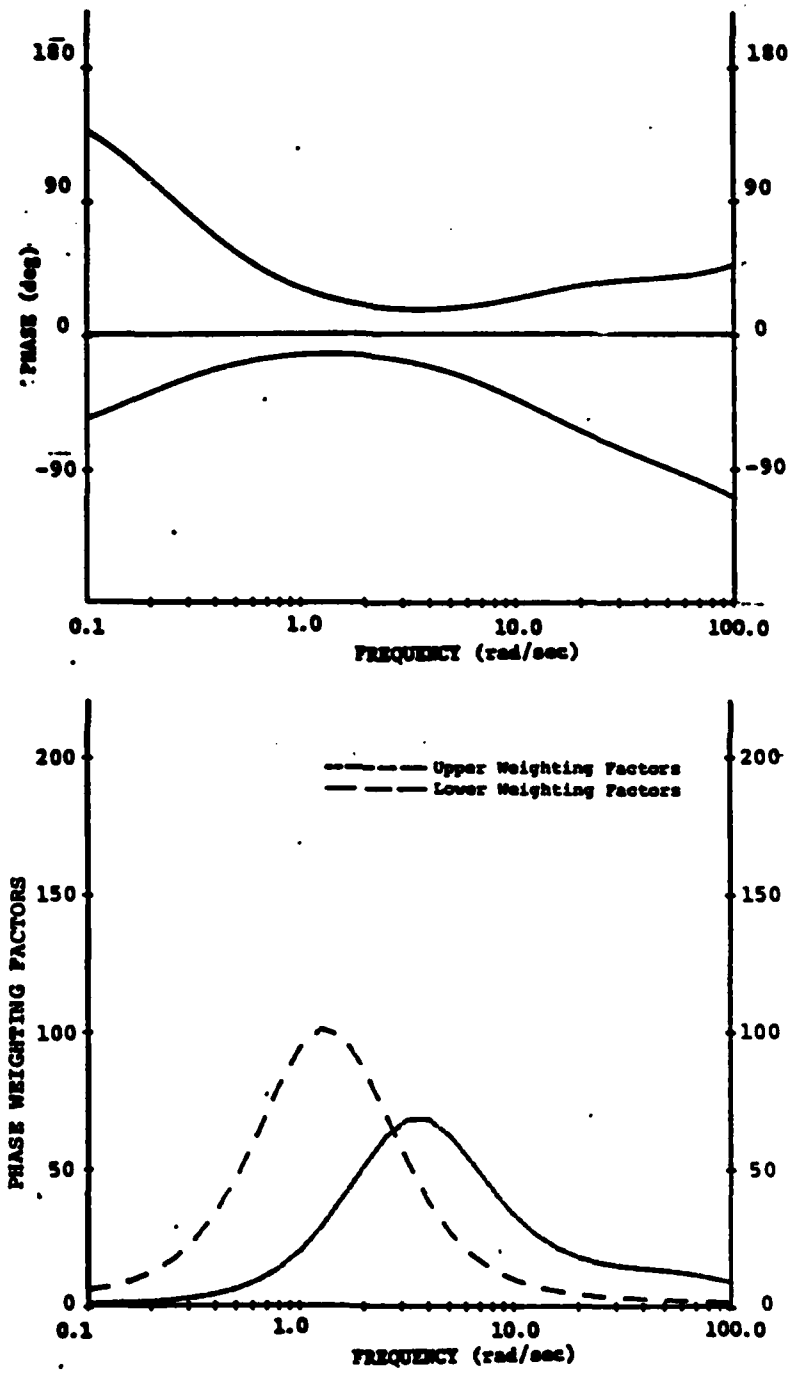

FIGURE 9 CTOL ENVELOPES OF MAXIMUM UNNOTICEABLE ADDED DYNAMICS (TRANSFER FUNCTIONS) AND ASSOCIATED WEIGHTING FACTORS (Cont'd)

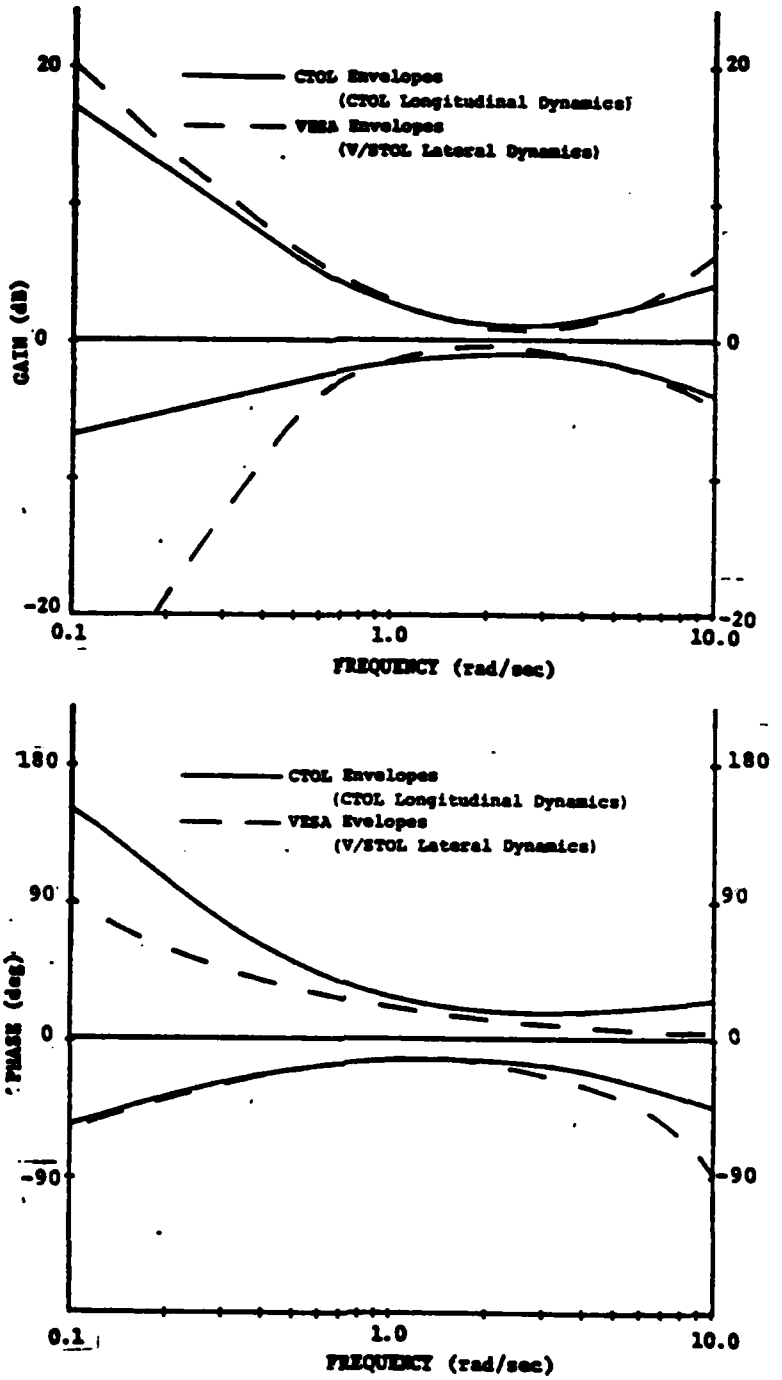

FIGURE 10 CTOL AND VESA ENVELOPES OF MAXIMUM UNNOTICEABLE ADDED DYNAMICS

APPENDIX A

DETERMINATION OF CTOL CRITICAL ADDED DYNAMICS

Appendix A establishes the dynamics used to form the envelopes of Maximum Unnoticeable Added Dynamics. The data sets from two conventional take-off and landing (CTOL), in-flight simulations were used to determine the effects on handling qualities of various types of added dynamics. Starting with the lowest order or "base" configurations from the Neal and Smith (Neal-Smith) and the Landing Approach High Order System (LAHOS) programs, the critical cases for the five types of added dynamics or additions (first order lead-lag, first order lag, second order lag prefilter, fourth order lag prefilter, and second order lag prefilter - first order lead-lag combination) were sought. The critical case is defined as the last set of added dynamics to produce no change in handling qualities or pilot rating with respect to those of the base configurations. The set of all critical cases is referred to as the critical added dynamics. Table A-1 defines all configurations in the two data sets, and Figure A-1 shows the block diagram of the configurations simulated.

Ideally enough data would be available to allow easy selection of a critical case for each type of addition (i.e., a finely varied matrix with progressively larger additions such that several unnoticeable additions would be followed by an addition that produces a definite degradation). To account for pilot rating scatter, an addition was considered unnoticeable if the worst degradation it caused was 0.5 (or less) on the Cooper-Harper scale. However the data sets were of limited size and there were no low frequency (below the crossover frequency) added dynamics. Sketches 1 and 2 (ΔGain Bode plots) illustrate the procedures used to find the critical cases for the various types of added dynamics.

The largest degradation for each lag in Sketch 1 was compared to the limit for unnoticeability (0.5) and Lags 1 and 2 were within the limit. Lag 3 was not, so Lag 2 is the critical case. Each set of added dynamics, including the critical cases,

will be referred to by the configuration it degraded the most. Configuration A-2 represents the Lag 2 critical case.

None of the lags shown in Sketch 2 were unnoticeable (within the 0.5 limit), again based on the worst degradation for each. Therefore no critical case actually exists (based on the definition given previously), and a replacement must be found. The first (highest frequency) dynamics of this type, Lag 4 here, will be used as the critical case and as before, will be referred to by the configuration with the worst degradation (Configuration C-4 for the data shown in Sketch 2).

The degradation will serve as a measure of how much an addition selected as a critical case differs from its definition; i.e., the smaller the degradation, the closer a "critical case" is to being truly unnoticeable. Because some "critical cases" actually are noticeable, any envelopes developed from them are not conservative; i.e., there is a possibility that a mismatch within the envelopes might be associated with a finite rating degradation.

EFFECTS OF LAHOS ADDED DYNAMICS

The LAHOS configurations were distributed among the five types of dynamics added to the base (-1) configurations as follows:

a) First order lead-lag (-A, -B, and -C);
b) First order lag (-2, -3, -4, and -5);
c) Second order lag prefilter (-6, -7, -8, -9, and -10);
d) Fourth order lag prefilter (-11); and
e) Second order lag prefilter - first order lead-lag combination (6-).

The last type represented the difference between the control systems of a modified YF-17 and the original YF-17. All configurations used the same feel system and actuator dynamics.

The LAHOS critical cases for the first order lead-lag, first order lag, and second order lag prefilter were the highest frequency added dynamics of that type. The critical case was represented by the configuration in this group having

SKETCH 1

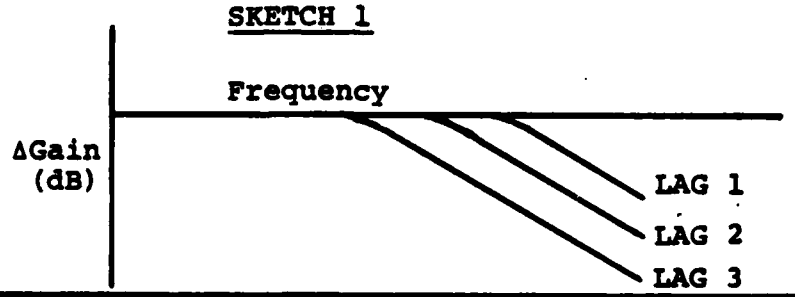

ADDED DYNAMICS	PILOT RATING DEGRADATION		
	[BASELINE]$_A$	[BASELINE]$_B$	[BASELINE]$_C$
LAG 1	A-1: 0.	B-1: 0.2	C-1: 0.1
LAG 2	A-2: 0.4	B-2: 0.	C-2: 0.1
LAG 3	A-3: 0.3	B-3: 0.1	C-3: 1.0

The data shown are qualitative and are not related to the data sets actually used, except in general format.

SKETCH 2

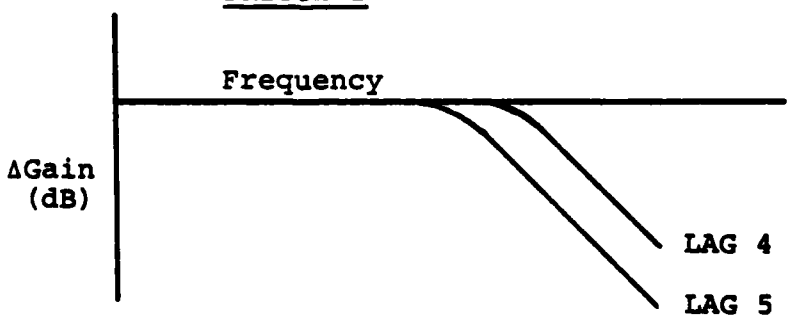

ADDED DYNAMICS	PILOT RATING DEGRADATION		
	[BASELINE]$_A$	[BASELINE]$_B$	[BASELINE]$_C$
LAG 4	A-4: 0.2	B-4: 0.7	C-4: 1.0
LAG 5	A-5: 0.8	B-5: 0	C-5: 1.0

The data shown are qualitative and are not related to the data sets actually used, except in general format.

the largest pilot rating degradation. For the other two types only one set of dynamics was used, and only the configuration with the largest degradation needed to be found.

The critical lead-lag case was represented by configuration 4-C, which suffered a degradation of 1.0 on the Cooper-Harper scale. The critical first order lag was represented by 2-2 with a degradation of 2.25. Although all -2 configurations caused degradations, 2-2 caused the largest. The critical case for second order lag prefilters was represented by 2-6 (degradation: 3) with the other -6 configurations having degradations raging from 0.0 to 1.2. Of the fourth order lag prefilter (-11) configurations, 2-11 and 4-11 had the largest degradation, 6. The second order lag prefilter - first order lead-lag combination caused a degradation of 8.

The frequency responses of the -C (first order lead-lag), -2 (first order lag) and -6 (second order lag prefilter) added dynamics were plotted on a common Bode plot to begin the process of constructing the MUAD envelopes. The -11 (fourth order lag prefilter) and YF-17 (second order lag prefilter - first order lead-lag combination) dynamics were not used due to the excessive degradations they caused. The LAHOS added dynamics are shown in Figures A-2 through A-15.

EFFECTS OF NEAL-SMITH ADDED DYNAMICS

The added dynamics used with the Neal-Smith base configurations (1D, 2D, 3A, 4A, 5A, 6C, 7C, and 8A) consisted of seven sets of first order lead-lag added dynamics and ten of first order lag dynamics. One set of lead-lag dynamics and two of lag dynamics were also run with a medium frequency Flight Control System (FCS) pole (ω_{FCS} = 16 rad/sec) instead of the high frequency FCS pole (ω_{FCS} = 63 rad/sec) used with the other sets. The high frequency pole had less effect on the frequency response of the added dynamics than the medium frequency pole, due to the base configurations' high frequency pole (ω_{FCS} = 75 rad/sec) nearly cancelling it out. The 63 rad/sec pole contributed approximately -3 dB of gain and 15 degrees of phase lag maximum at high frequencies, while the 16 rad/sec pole added -26 dB of gain and 100

degrees of phase lag.

Configuration 2C represented the critical first order lead-lag case, causing a degradation of 0.33. Lead-lag configuration 7B was also considered unnoticeable with a degradation of 0.12. Configuration 7D represented the critical first order lag case with a degradation of 2.62.

The frequency responses of the 2C (first order lead-lag) and 7D (first order lag) added dynamics were plotted with the LAHOS critical cases to aid in constructing the MUAD envelopes. Although the 2C added dynamics were the critical lead-lag case, the unnoticeable 7B dynamics allowed larger phase mismatches at high frequencies. This indicated, at least for the upper phase curve, the envelopes do not "neck down" at high frequencies. The Neal-Smith added dynamics are shown in Figures A-16 through A-32.

The critical cases, Figure A-33, chosen in this appendix are used in Appendix B to shape envelopes of Maximum Unnoticeable Added Dynamics. The Maximum Unnoticeable Added Dynamics is the largest amount of added dynamics that can be added to a low order system without the pilot noticing a change in handling qualities. This is theoretically quite different from the Minimum Noticeable Added Dynamics, which is the smallest amount of added dynamics that the pilot will notice. However when examining real test data, the difference is hard to establish due to the limited amount of available data, and the Minimum Noticeable Added Dynamics must sometimes be used instead of Maximum Unnoticeable Added Dynamics. Figure A-34 shows the difference between the Maximum Unnoticeable and Minimum Noticeable Added Dynamics.

Landing Approach High Order System (LAHOS) Dynamics

Data in blocks refer to: CONFIGURATION/AVERAGE PR

CONTROL SYSTEM DYNAMICS					SHORT PERIOD DYNAMICS (nominal) V_{ind} = 120 Kt; n/α = 4.5 g/rad; $1/\tau_{\theta_2}$ = .7143 sec^{-1}				
					ω_{SP}/ζ_{SP}				
$1/\tau_1$	$1/\tau_2$	ω_{FCS}/ζ_{FCS}	ω_3/ζ_3	ω_4/ζ_4	1.0/.74	2.3/.57	2.2/.25	2.0/1.06	3.9/.54
2.5	10	75/.7	-	-	1-A / 6	2-A / 5			
3.3	↓	↓	-	-	1-B / 5				
5	↓	↓	-	-	1-C / 4	2-C / 2.5	3-C / 3.5	4-C / 3	
↓	=	↓	-	-	1-1 / 4	2-1 / 2	3-1 / 5.3	4-1 / 2	5-1 / 6
↓	10	↓	-	-	1-2 / 5	2-2 / 4.25	3-2 / 7		
↓	4	↓	-	-	1-3 / 9.5	2-3 / 6	3-3 / 10	4-3 / 6.7	5-3 / 6.2
↓	2	↓	-	-	1-4 / 10	2-4 / 9		4-4 / 6.5	5-4 / 6
↓	1	↓	-	-					5-5 / 7
↓	=	↓	16/.7	-	1-6 / 5	2-6 / 5	3-6 / 6.5	4-6 / 4	5-6 / 6
↓	↓	↓	12/.7	-		2-7 / 6.5	3-7 / 8	4-7 / 3	5-7 / 6
↓	↓	↓	9/.7	-	1-8 / 8				
↓	↓	↓	6/.7	-		2-9 / 10			
↓	↓	↓	4/.7	-		2-10 / 10		4-10 / 9	
↓	↓	↓	16/.93	16/.38	1-11 / 9	2-11 / 8		4-11 / 8	5-11 / 7

CONFIG./PR	CONTROL SYSTEM DYNAMICS	ω_{SP}/ζ_{SP}	ω_{FCS}/ζ_{FCS}
6-1 / 10 (YF-17 Original)	$\frac{(.5S+1)(.43S+1)}{(.2S+1)(1.1S+1)\left(\frac{S^2}{4^2}+\frac{2(.7)}{4}S+1\right)}$	1.9/.65	75/.7
6-2 / 2 (YF-17 Modified)	$\frac{(.5S+1)(.43S+1)(.065+1)}{(.2S+1)(.1S+1)(1.1S+1)}$	1.9/.65	75/.7

NOTES:

(1) First number indicates base aircraft configuration simulated; second number or letter identifies control system dynamics; letters for control system lead-lag; numbers for lag.

(2) Total configuration dynamic model includes feel system dynamics:

$$\frac{\delta_s}{F_s} = \frac{.125}{\frac{S^2}{(26)^2}+\frac{2(.6)S}{26}+1} \quad \text{(in/lb)}$$

(3) Adapted from Reference 10.

Table A-1 Nominal LAHOS and Neal-Smith Control System Dynamics

Neal and Smith (Neal-Smith) Dynamics

Data in blocks refer to: CONFIGURATION/AVERAGE FR

CONTROL SYSTEM DYNAMICS			SHORT PERIOD DYNAMICS (Nominal)							
			V_{ind} = 250 Kt; n/α = 18.5 g/rad; $1/\tau_{\theta_2}$ = 1.25 sec^{-1}					V_{ind} = 350 Kt; n/α = 50g/rad; $1/\tau_{\theta_2}$ = 2.4 sec^{-1}		
			ω_{SP}/ζ_{SP}					ω_{SP}/ζ_{SP}		
$1/\tau_1$	$1/\tau_2$	ω_{FSC}/ζ_{FSC}	2.2 / .69	4.9 / .70	9.7 / .63	5.0 / .28	5.1 / .18	3.4 / .67	7.3 / .73	16.5 / .69
0.5	2	63 / .75	1A / 5							
0.8	3.3							6A / 5.5		
2	5		1B / 3.25	2A / 4.25						
3.3	8							6B / 2.5	7A / 3.67	
5	12			2C / 3						
8	19								7B / 3	
∞	∞	75 / .67	1D / 4.13	2D / 2.67	3A / 4.25	4A / 5.25	5A / 6	6C / 4.5	7C / 2.88	8A / 4.5
	19	63 / .75							7D / 5.5	8B / 3.5
	12			2E / 4	3B / 4.5	4B / 7	5B / 7			
	8							6D / 5.5	7E / 5.5	8C / 3.25
	5		1E / 6	2F / 5.67	3C / 3.5	4C / 8.5	5C / 8			
	3.3							6E / 7.75	7F / 5.11	8D / 3
	2		1F / 8	2H / 5.5	3D / 4	4D / 8.5	5D / 8.83		7G / 5.5	
	0.8							6F / 8.83	7H / 5	8E / 3.5
	0.5		1G / 8.5	2I / 6	3E / 4	4E / 7.5	5E / 8			
2	5	16 / .75	1C / 4.17	2B / 5.25						
	5			2G / 7						
	2			2I / 8						

NOTES:

(1) Number indicates base aircraft configuration simulated; letter identifies control system dynamics.

(2) Total configuration dynamic model includes feel system dynamics:

$$\frac{\delta_s}{F_s} = \frac{.046}{\frac{S^2}{(31)^2} + \frac{2(1.0)S}{31} + 1} \quad \text{(in/lb)}$$

(3) Adapted from Reference 8.

Table A-1 Nominal LAHOS and Neal-Smith Control System Dynamics (cont'd)

LAHOS BLOCK DIAGRAM

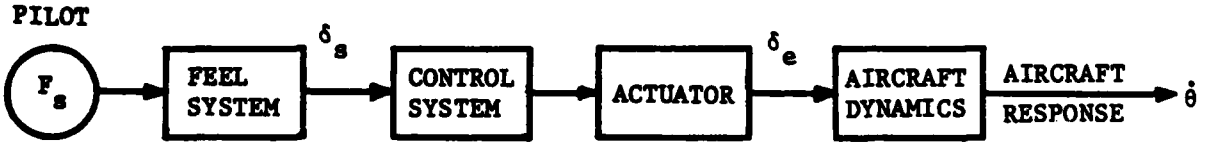

NEAL-SMITH BLOCK DIAGRAM

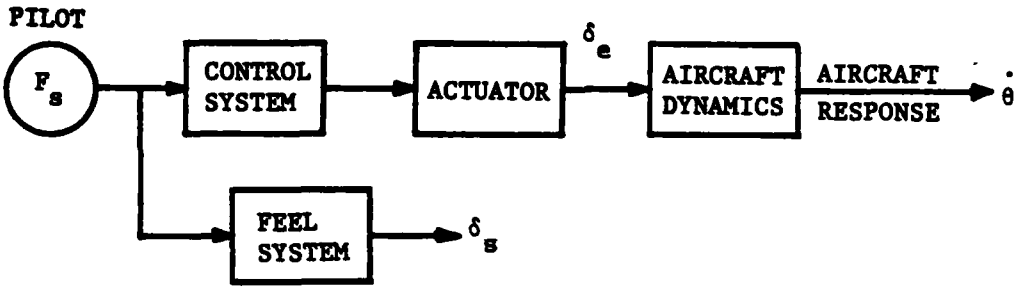

Feel System:

$$\frac{\delta_s}{F_s} = \frac{K_{FS}}{\frac{S^2}{\omega_{FS}^2} + \frac{2\zeta_{FS}S}{\omega_{FS}} + 1}$$

Control System:[1]

$$\frac{\tau_1 S+1}{(\tau_2 S+1)\left(\frac{S^2}{\omega_3^2} + \frac{2\zeta_3 S}{\omega_3} + 1\right)\left(\frac{S^2}{\omega_4^2} + \frac{2\zeta_4 S}{\omega_4} + 1\right)}$$

Actuator:

$$\frac{1}{\frac{S^2}{\omega_{FCS}^2} + \frac{2\zeta_{FCS}S}{\omega_{FCS}} + 1}$$

Aircraft Dynamics:

$$K_{\dot{\theta}} \frac{T_{\theta_2} S+1}{\frac{S^2}{\omega_{SP}^2} + \frac{2\zeta_{SP}S}{\omega_{SP}} + 1} = K_{\dot{\theta}} \frac{\frac{S}{L_\alpha} + 1}{\frac{S^2}{\omega_{SP}^2} + \frac{2\zeta_{SP}S}{\omega_{SP}} + 1}$$

[1]Configurations 6-1 and 6-2 had different Control System dynamics (up to two first order numerator roots and two first order denominator roots in addition to what is already shown).

Figure A-1 Block Diagram for Configurations Simulated

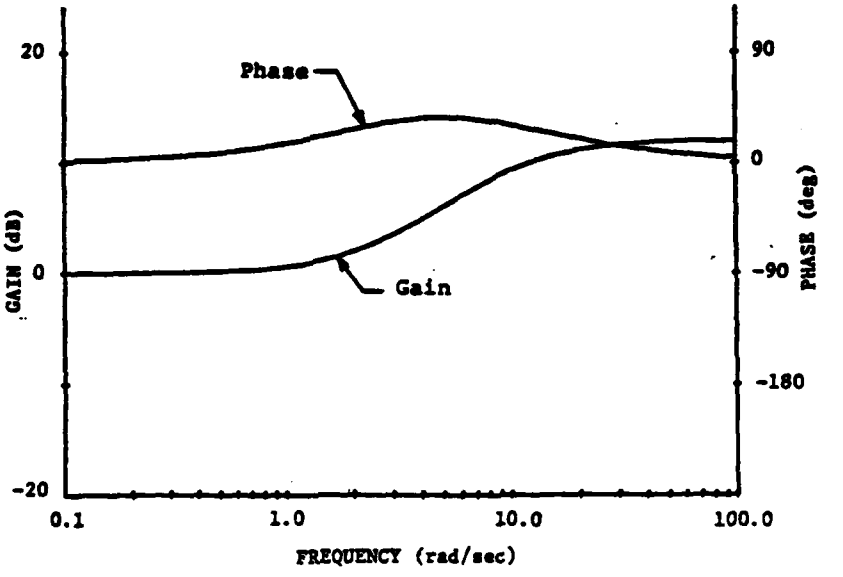

-A LAHOS Added Dynamics

FIGURE A-2

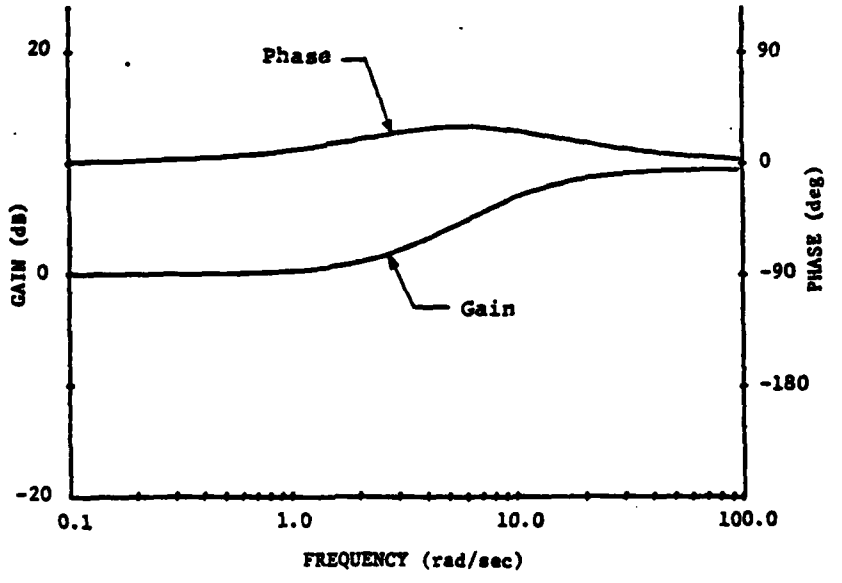

-B LAHOS Added Dynamics

FIGURE A-3

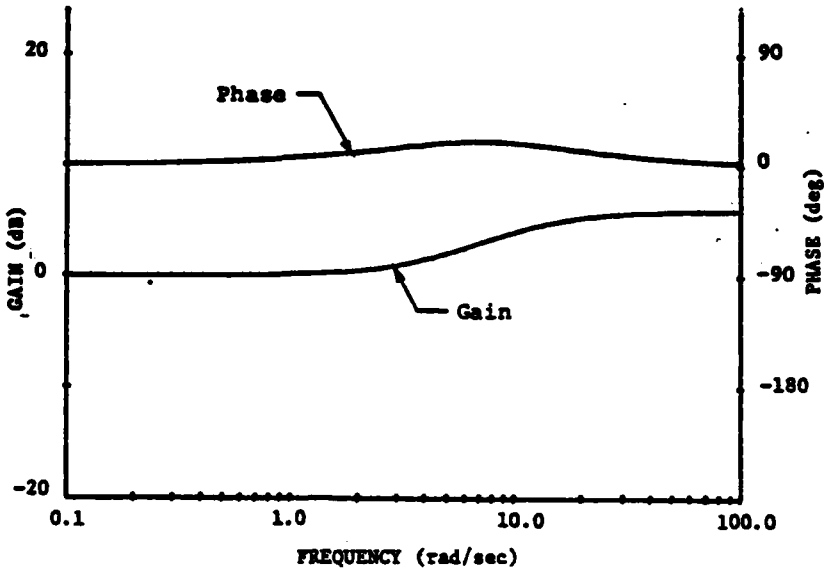

-C LAHOS Added Dynamics

FIGURE A-4

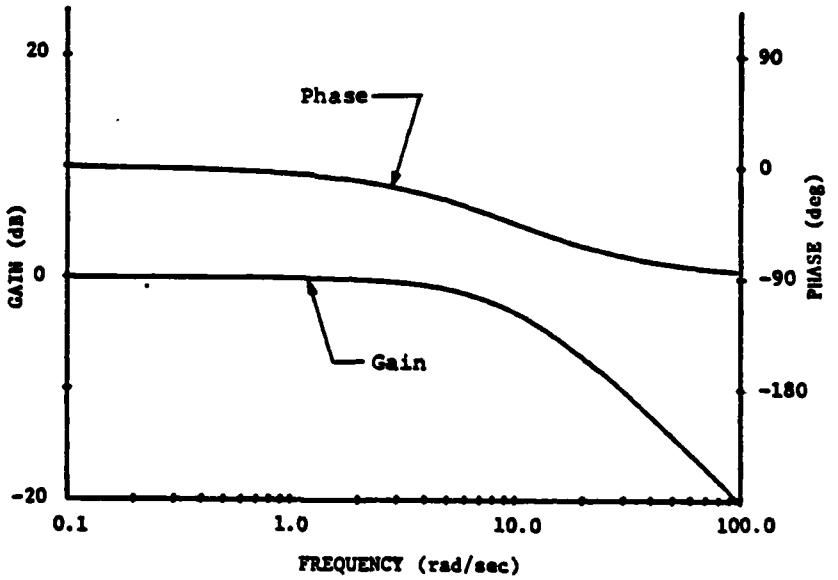

-2 LAHOS Added Dynamics

FIGURE A-5

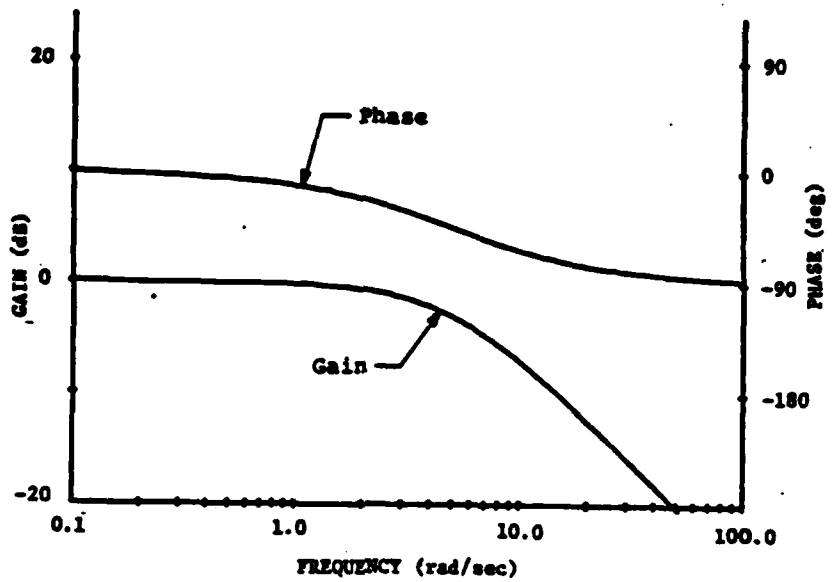

-3 LAHOS Added Dynamics

FIGURE A-6

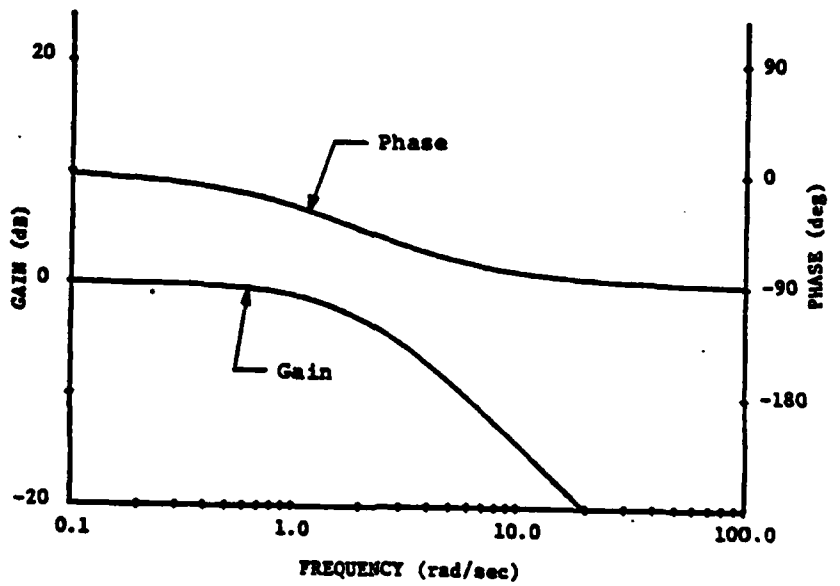

-4 LAHOS Added Dynamics

FIGURE A-7

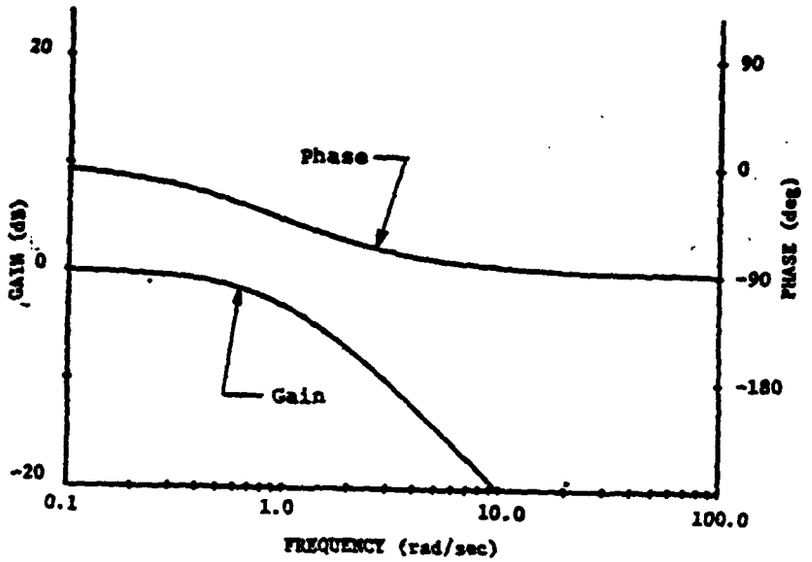

-5 LAHOS Added Dynamics

Figure A-8

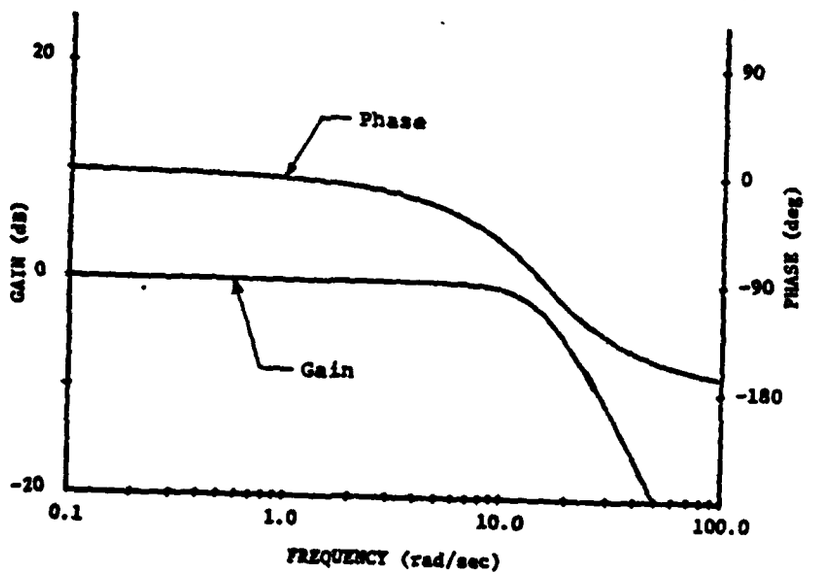

-6 LAHOS Added Dynamics

FIGURE A-9

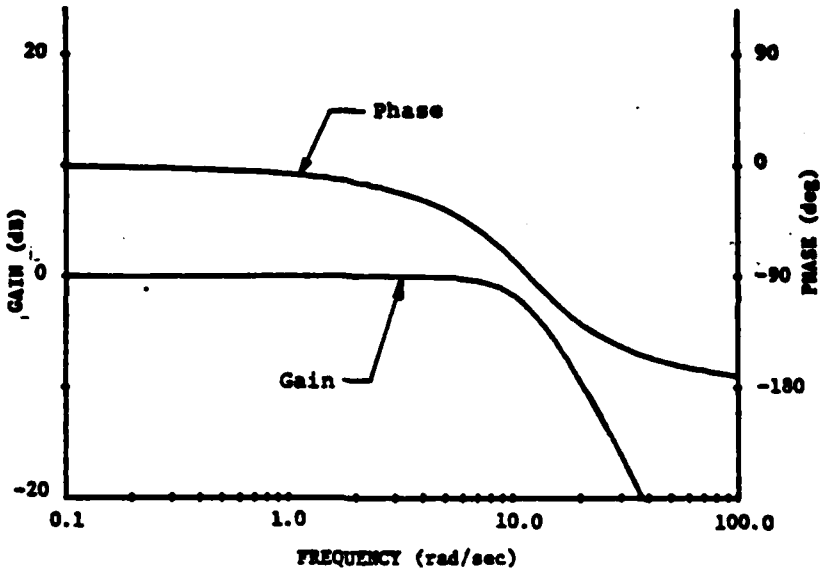

-7 LAHOS Added Dynamics

FIGURE A-10

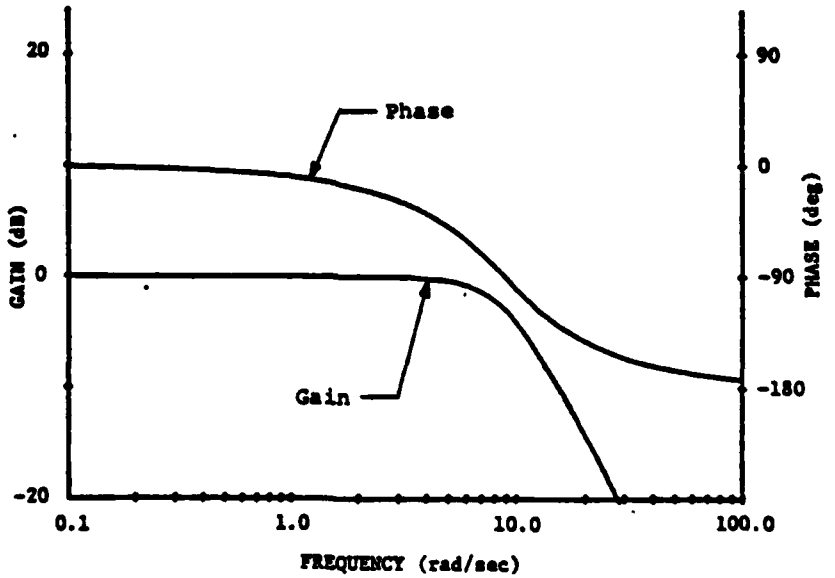

-8 LAHOS Added Dynamics

FIGURE A-11

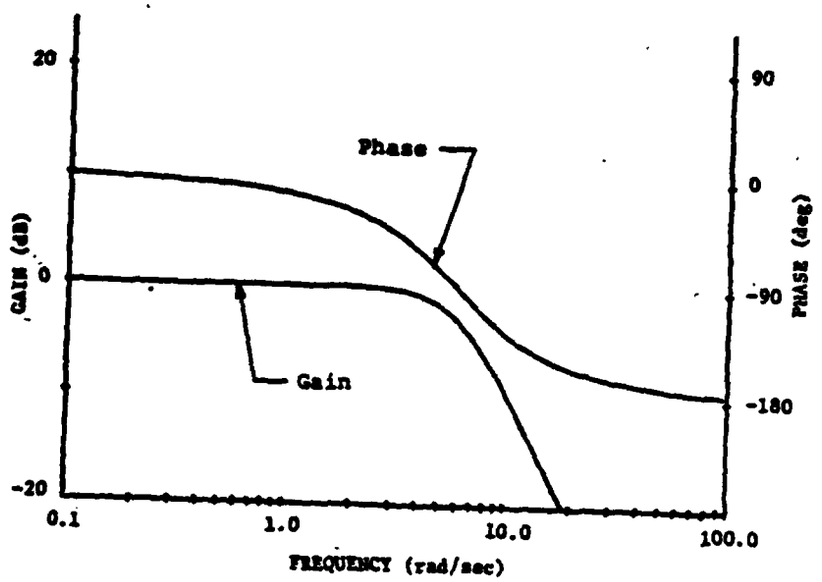

-9 LAHOS Added Dynamics

FIGURE A-12

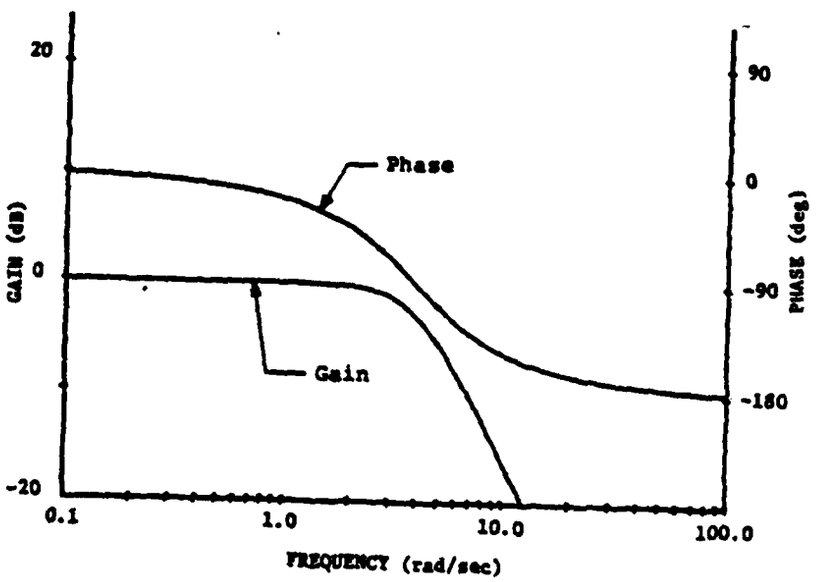

-10 LAHOS Added Dynamics

FIGURE A-13

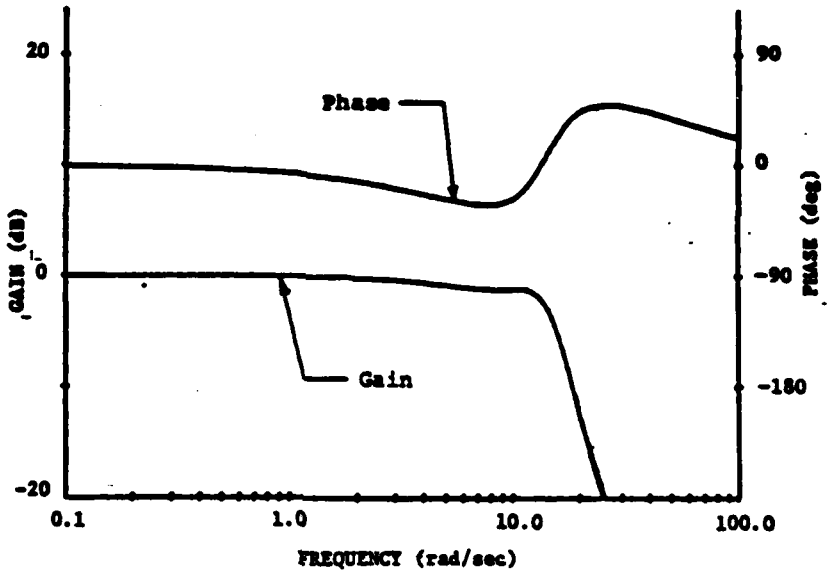

-11 LAHOS Added Dynamics

FIGURE A-14

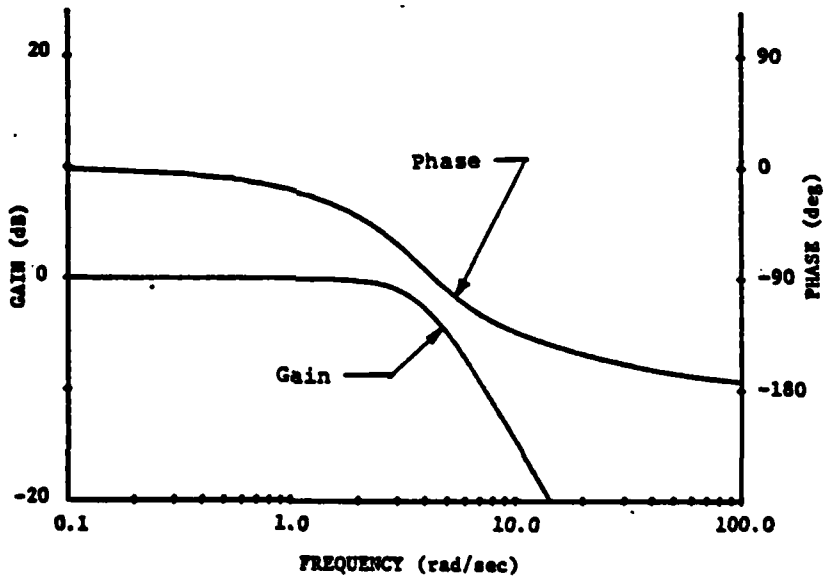

YF-17 LAHOS Added Dynamics

FIGURE A-15

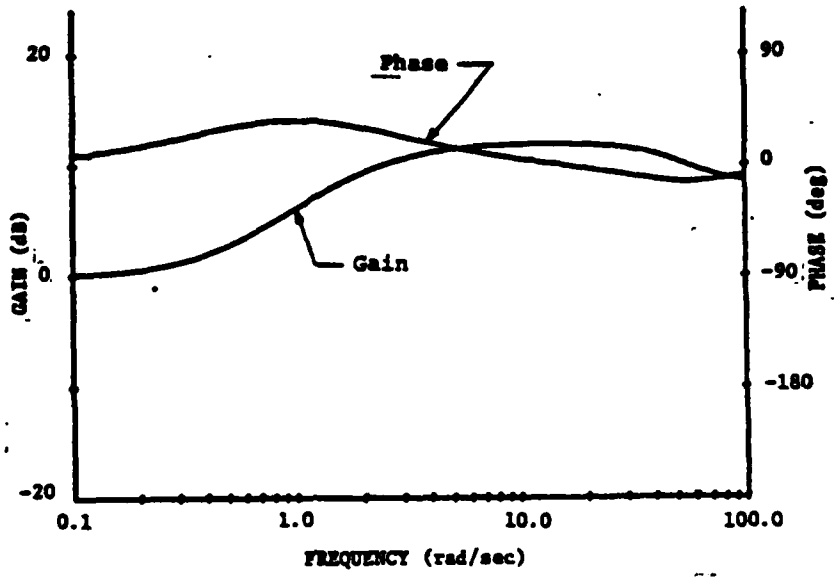

1A Neal-Smith Added Dynamics

FIGURE A-16

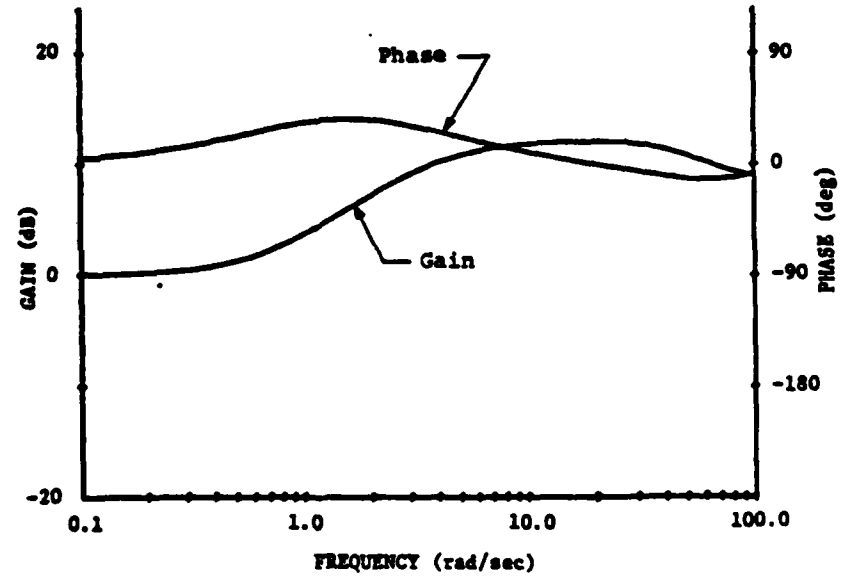

6A Neal-Smith Added Dynamics

FIGURE A-17

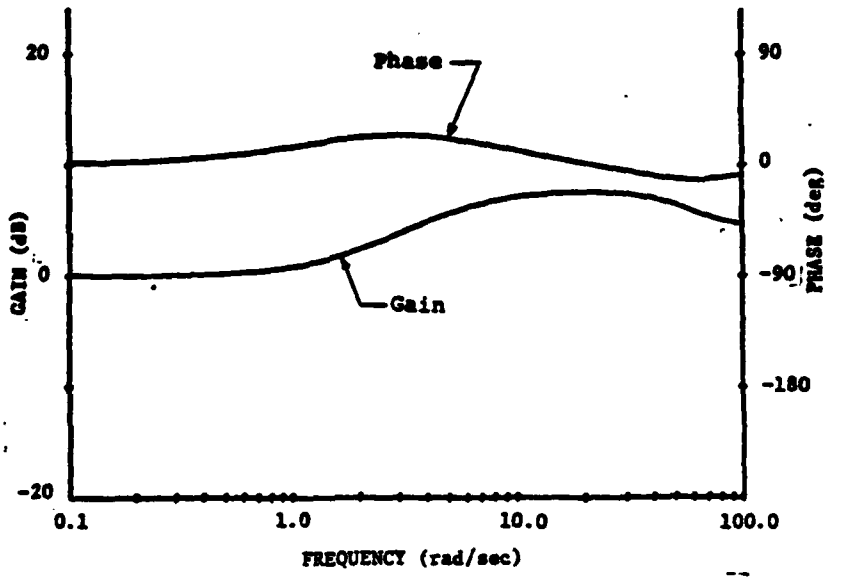

1B,2A Neal-Smith Added Dynamics

FIGURE A-18

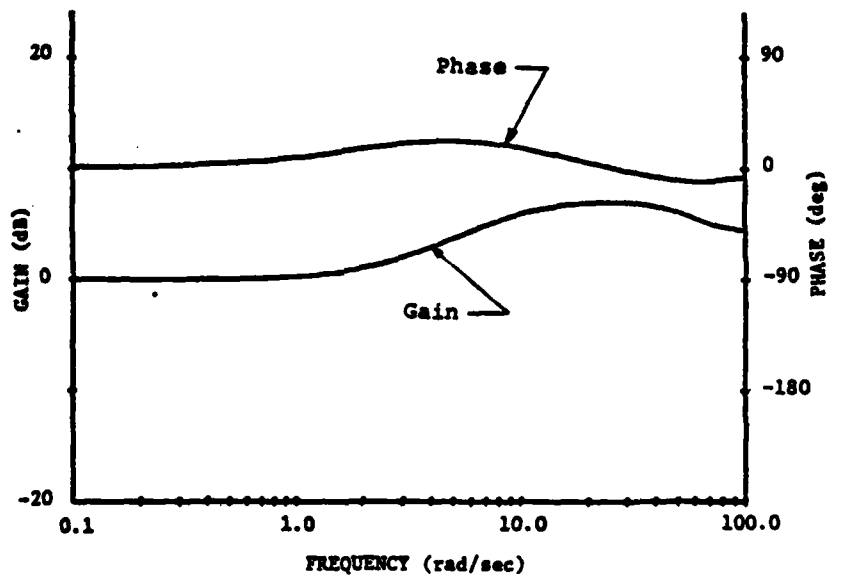

6B,7A Neal-Smith Added Dynamics

FIGURE A-19

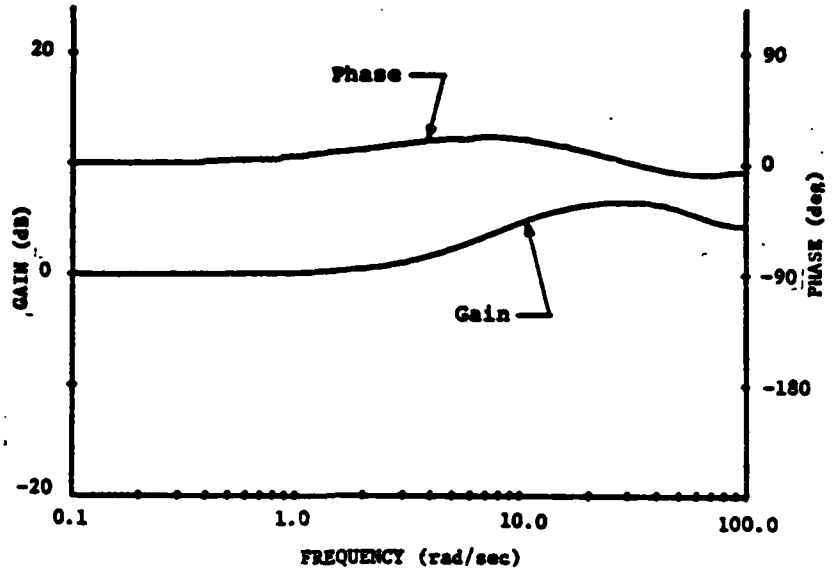

2C Neal-Smith Added Dynamics

FIGURE A-20

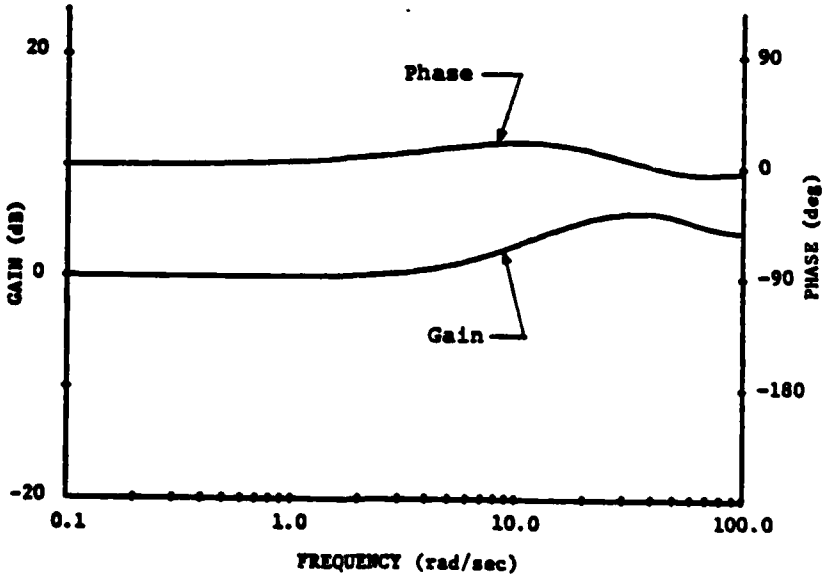

7B Neal-Smith Added Dynamics

FIGURE A-21

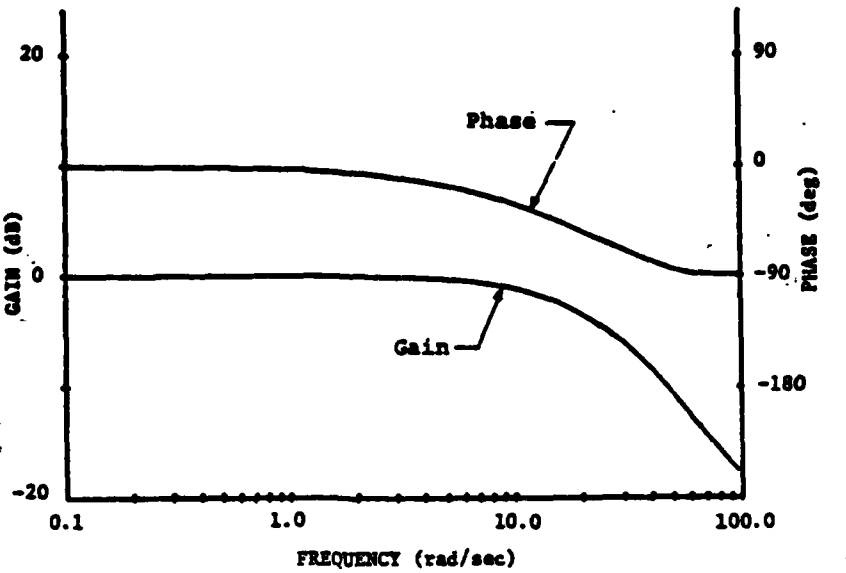

7D,8B Neal-Smith Added Dynamics

FIGURE A-22

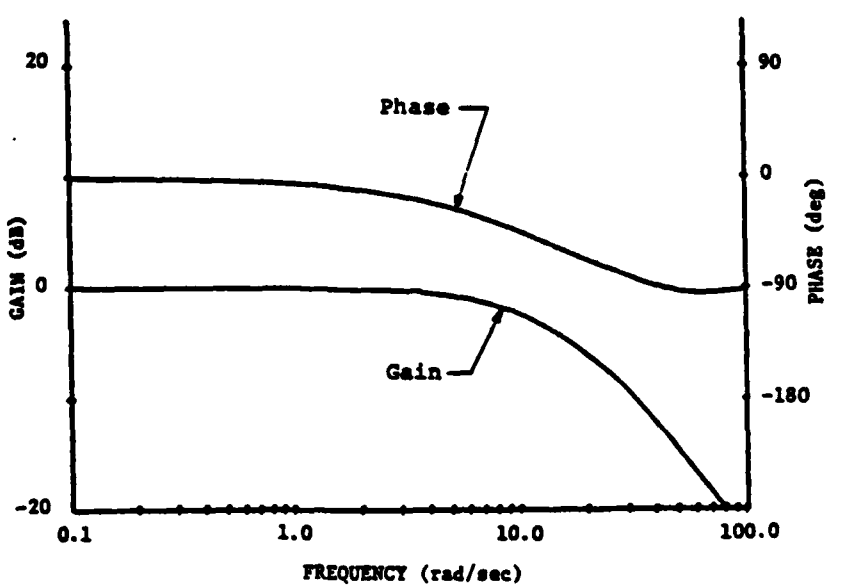

2E,3B,4B,5B Neal-Smith Added Dynamics

FIGURE A-23

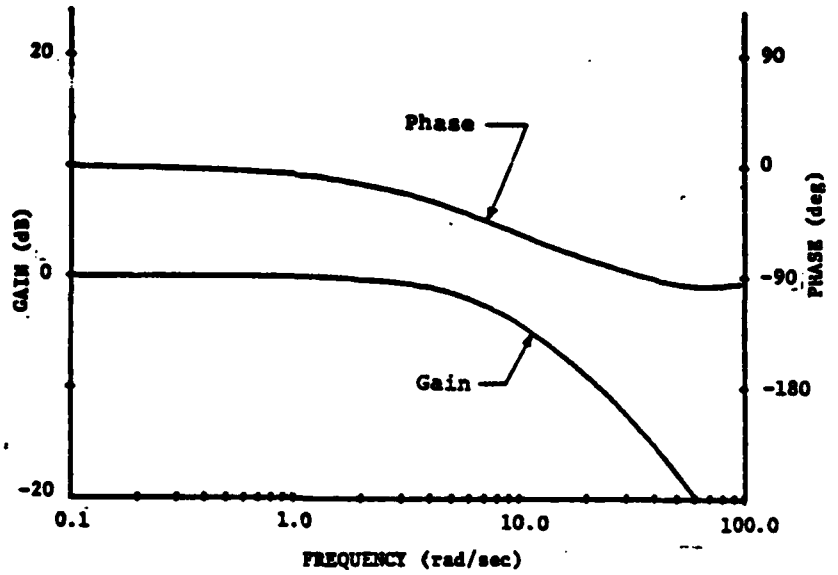

6D,7E,8C Neal-Smith Added Dynamics

FIGURE A-24

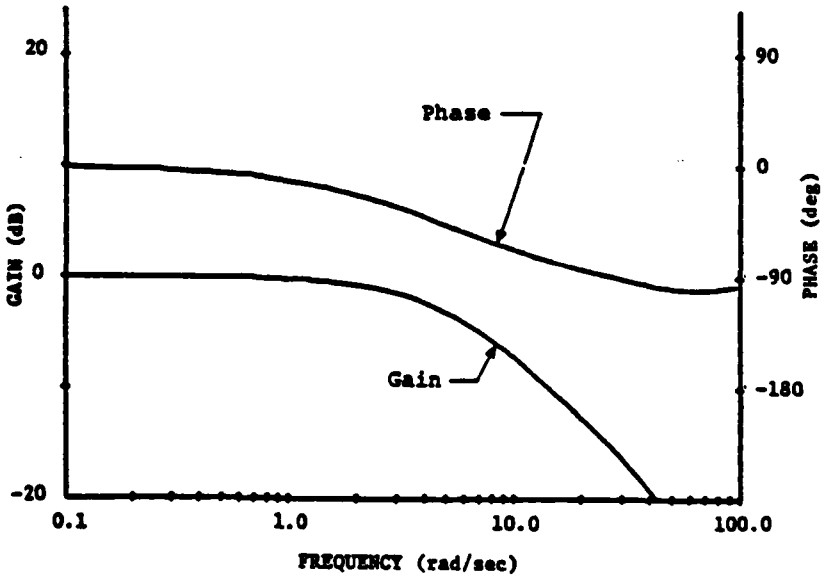

1E,2F,3C,4C,5C Neal-Smith Added Dynamics

FIGURE A-25

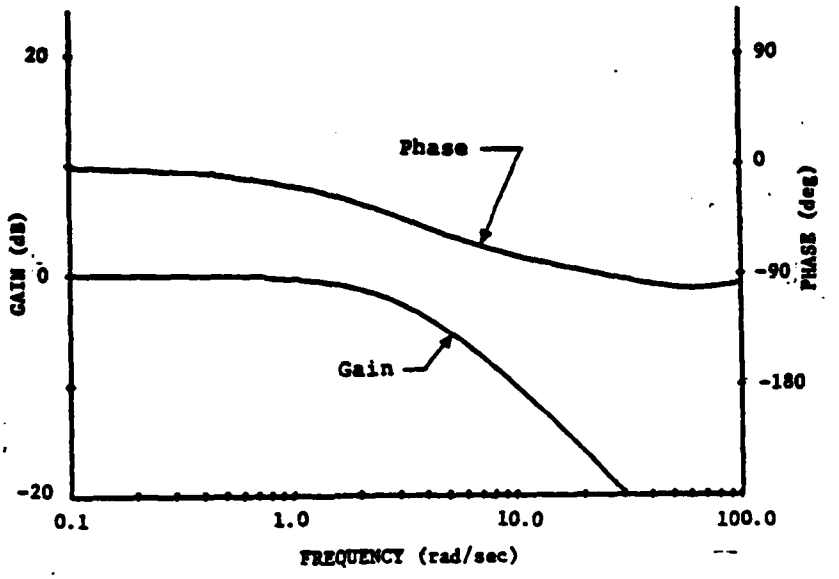

6E,7F,8D Neal-Smith Added Dynamics

FIGURE A-26

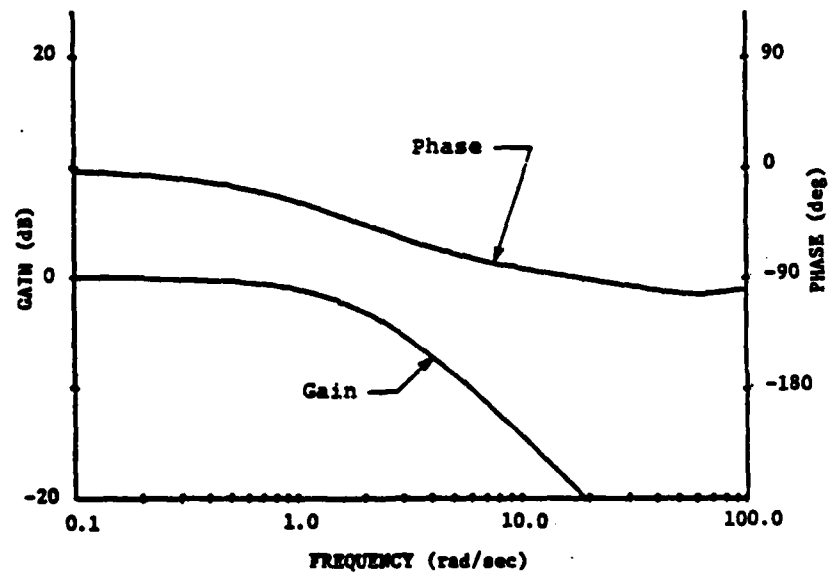

1F,2H,3D,4D,5D,7G Neal-Smith Added Dynamics

FIGURE A-27

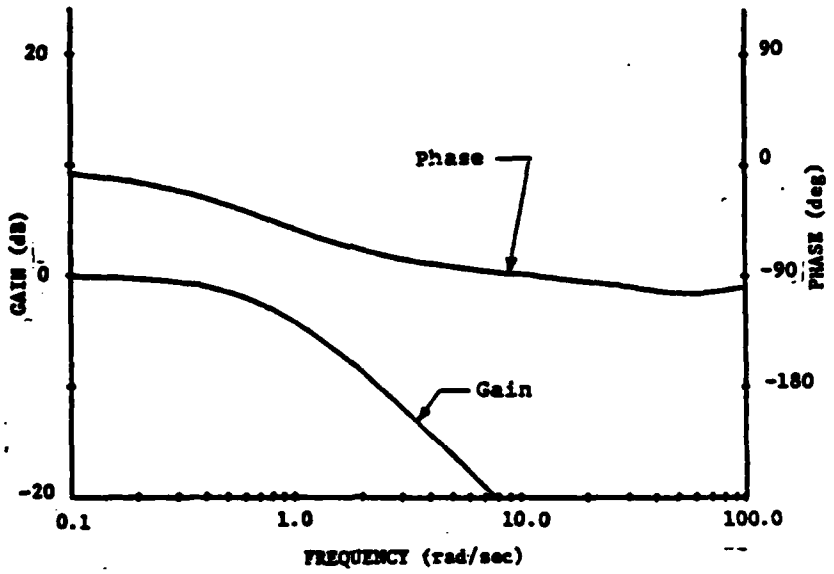

6F,7H,8E Neal-Smith Added Dynamics

FIGURE A-28

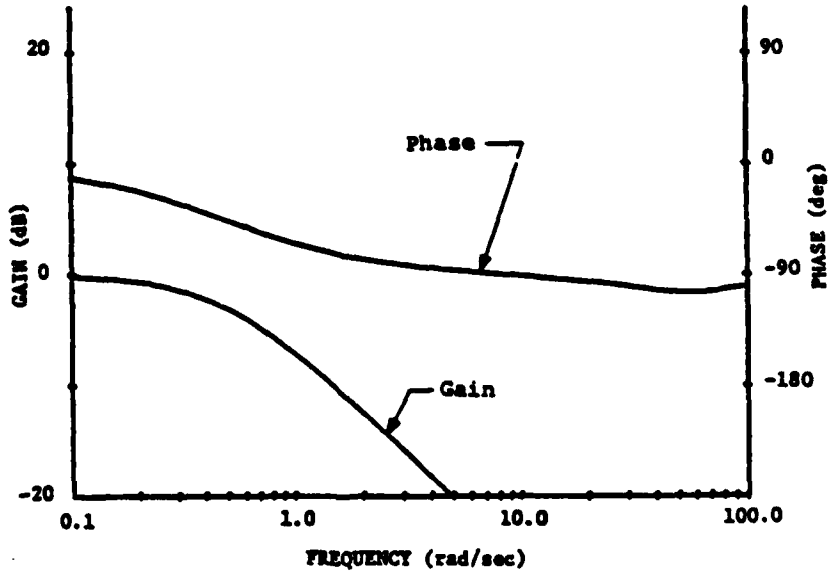

1G,2J,3E,4E,5E Neal-Smith Added Dynamics

FIGURE A-29

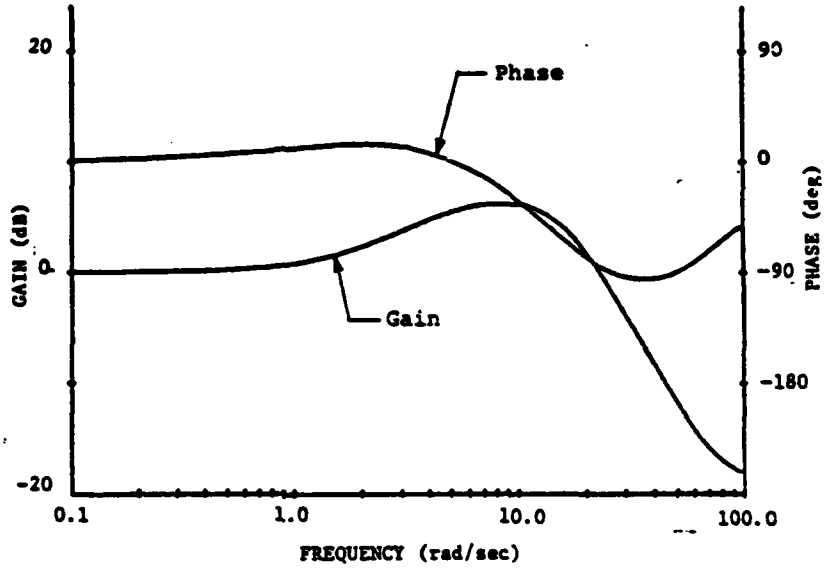

1C, 2B Neal-Smith Added Dynamics

FIGURE A-30

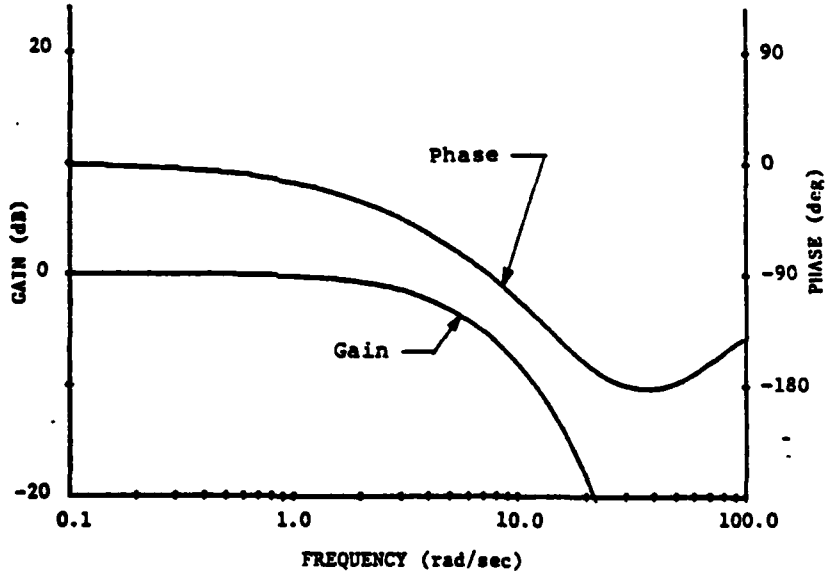

2G Neal-Smith Added Dynamics

FIGURE A-31

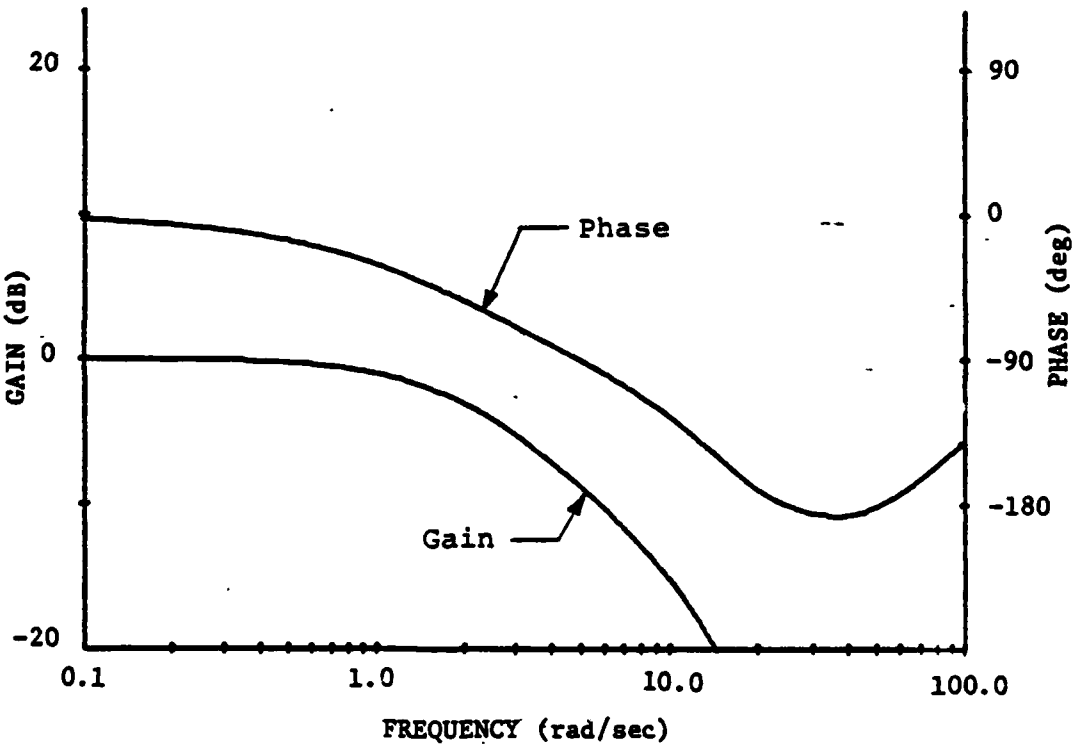

2I Neal-Smith Added Dynamics

FIGURE A-32

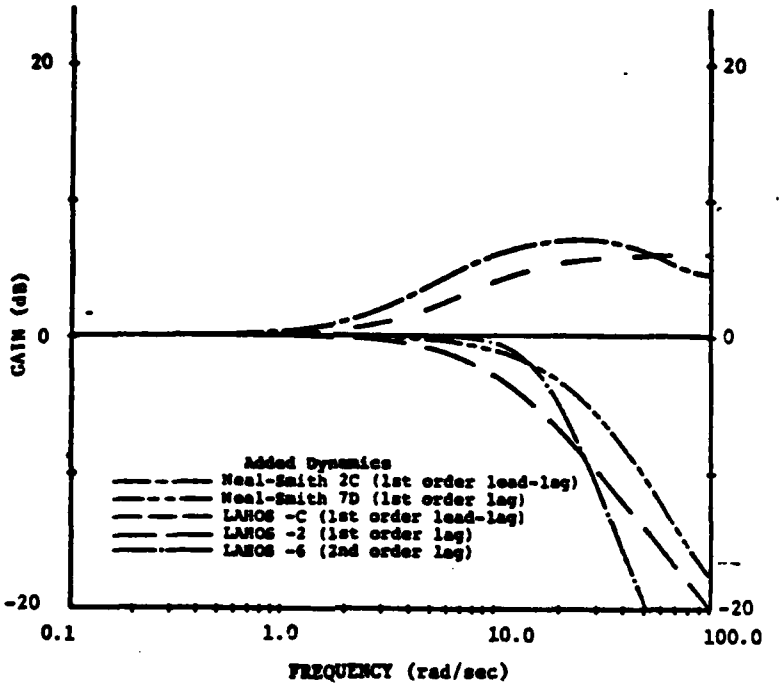

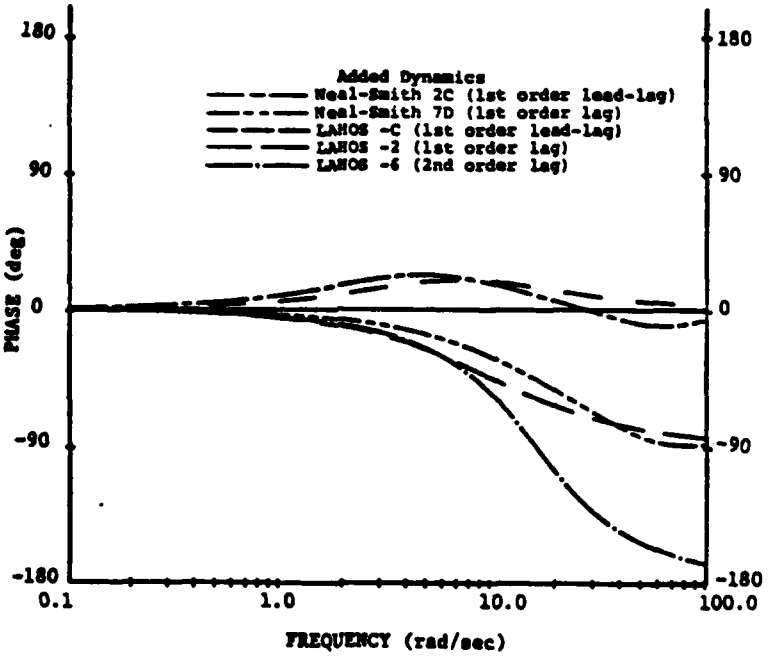

FIGURE A-33 Neal-Smith and LAHOS Critical Added Dynamics

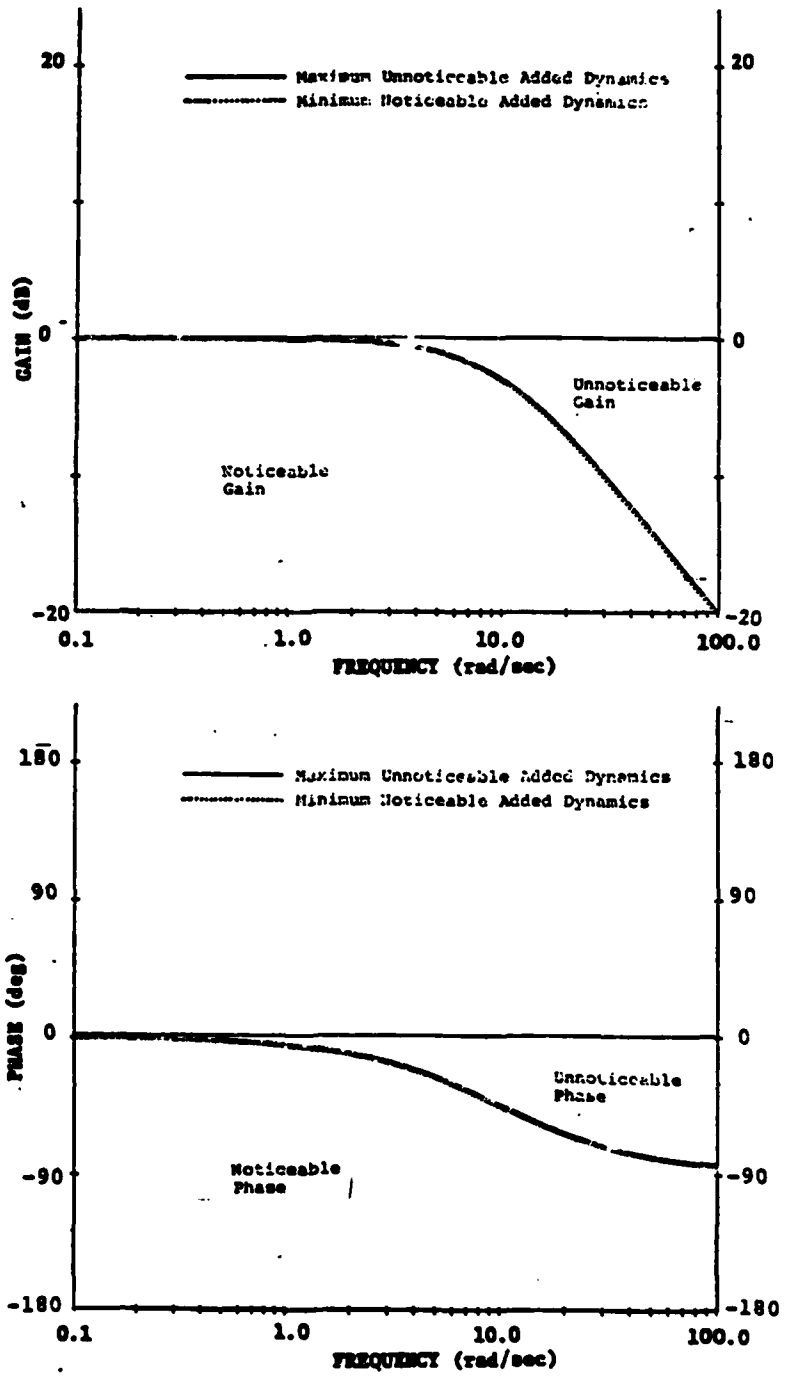

FIGURE A-34 Definition of Maximum Unnoticeable and Minimum Noticeable Added Dynamics

APPENDIX B

CTOL ENVELOPES OF MAXIMUM UNNOTICEABLE ADDED DYNAMICS

Appendix B describes the CTOL envelopes of Maximum Unnoticeable Added Dynamics developed from the LAHOS and Neal-Smith critical added dynamics, the matching procedure used to obtain transfer function matches for the CTOL envelopes, and the reasoning behind that procedure.

Once all of the critical cases have been found, partial envelopes of Maximum Unnoticeable Added Dynamics enclosing them may be drawn. The partial envelopes would enclose high frequency dynamics only and therefore be extremely narrow in the low frequency range. In the VESA study, both high and low frequency added dynamics were used and this provided wide low frequency envelopes. The LAHOS phugoid transfer function:

$$\frac{\dot{\theta}}{F_s} = \frac{S(S + 1/T_{\theta_1})}{S^2 + 2\zeta_p\omega_p S + \omega_p^2}: \quad T_{\theta_1} = 11.77;\ \omega_p = .196;\ \zeta_p = .135$$

was added to the Neal-Smith and LAHOS critical cases (high frequency) to introduce low frequency effects. Envelopes including both high and low frequency dynamics were then drawn, Figures B-1 through B-4, based on the VESA envelopes. The envelopes were input in tabular form (gain or phase versus frequency) to an interactive frequency response matching program (NAVFIT) to obtain transfer functions that match either a gain or phase envelope curve (upper or lower) from 0.1 to 100 rad/sec.

Using a second over second order (2/2) system, the initial match run for each curve was made with low order time delay fixed at zero and negative coefficients not allowed. For the same order system, the time delay and coefficient signs were allowed to vary if a satisfactory match (mismatch less than 5) was not obtained on the initial run. If a satisfactory match still was not obtained, the system order was varied and the procedure repeated until one was obtained.

For the Upper Gain Envelope, a 2/2 system with the time delay fixed, positive coeffients, and a mismatch of 2.525 was chosen. The 2/2 system with time delay free and negative coefficients allowed also had a mismatch of 2.525; and a 3/3 system with time delay free and negative coefficients allowed had a mismatch of 2.455. These systems were not chosen because the initial 2/2 system was simpler although the 3/3 system's mismatch was slightly smaller. For the Lower Gain Envelope, 2/2 systems with time delay fixed - positive coefficients, and time delay free - negative coefficients allowed were examined and found to have identical mismatches of 1.607. Using the same reasoning as before, the time delay fixed - positive coefficient system was chosen.

The Lower Phase Envelope was matched best by a time delay free - positive coefficient 2/2 system (mismatch = .109). A similar system with time delay fixed gave a mismatch of 46. The best match obtained for the Upper Phase Envelope had a mismatch of 96. This was an unsatisfactory match and the proposed envelope was revised. The best match for the revised envelope had a better but still unsatisfactory, mismatch of 14.6. After a second revision, the mismatch for a time delay free - negative coefficient allowed 2/2 system was 4.8, a satisfactory match.

The transfer functions, obtained as a result of the matches, describe the gain and phase envelopes accurately and are more compact than tables. However, the major advantage of the transfer functions, and the reason they were found, is that any frequency range may be used with them. If the envelope tables were used, all matches would have to be performed at the frequencies used in the tables. With the transfer functions, the gain and phase envelopes can be calculated for any frequency range and any frequencies in that range. However, the transfer functions should be used between .1 and 100 rad/sec, because the envelopes were originally drawn, tabulated, and then matched to transfer functions within these limits. The transfer functions may be used outside the .1 to 100 rad/sec range if the match beyond it is checked, and if necessary new transfer functions calculated. The envelope transfer functions are:

Upper Gain Envelope:

$$\frac{3.16S^2 + 31.61S + 22.79}{S^2 + 27.14S + 1.84}$$

Lower Gain Envelope:

$$\frac{9.55E\text{-}2S^2 + 9.92S + 2.15}{S^2 + 11.60S + 4.95}$$

Upper Phase Envelope:

$$\frac{68.89S^2 + 1100.12S - 275.22}{S^2 + 39.94S + 9.99} e^{.0059S}$$

Lower Phase Envelope:

$$\frac{475.32S^2 + 184100S + 29456.1}{S^2 + 11.66S + 3.89E\text{-}2} e^{-.0072S}$$

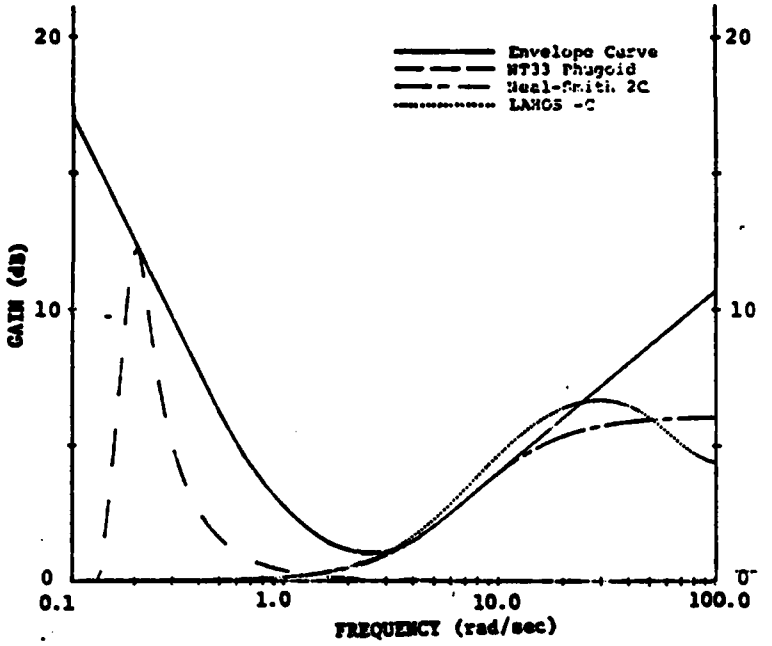

Figure B-1 Upper Gain Envelope and Critical Added Dynamics

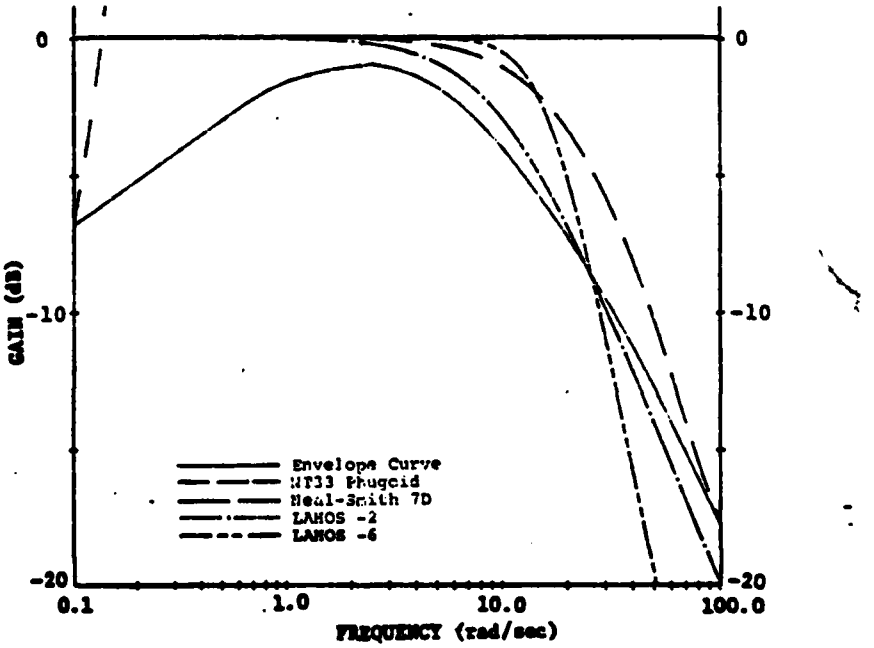

Figure B-2 Lower Gain Envelope and Critical Added Dynamics

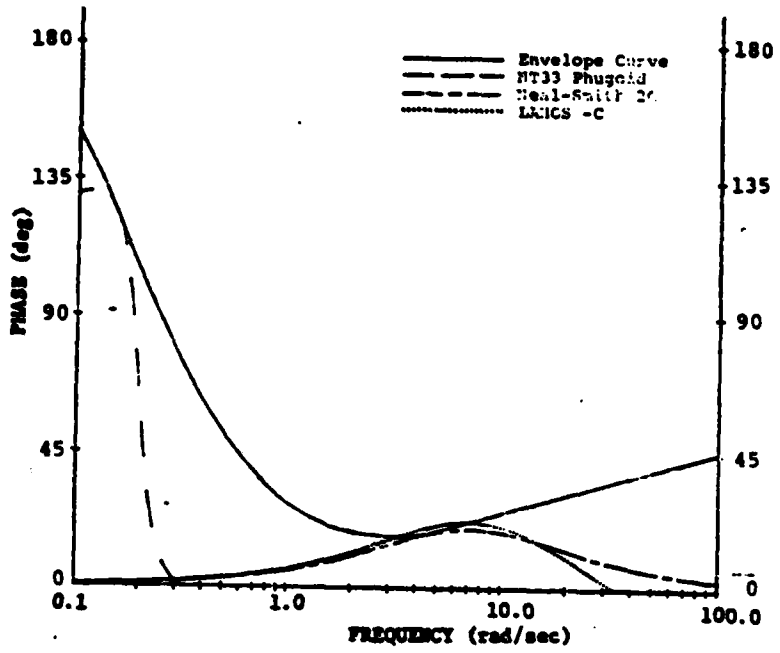

Figure B-3 Upper Phase Envelope and Critical Added Dynamics

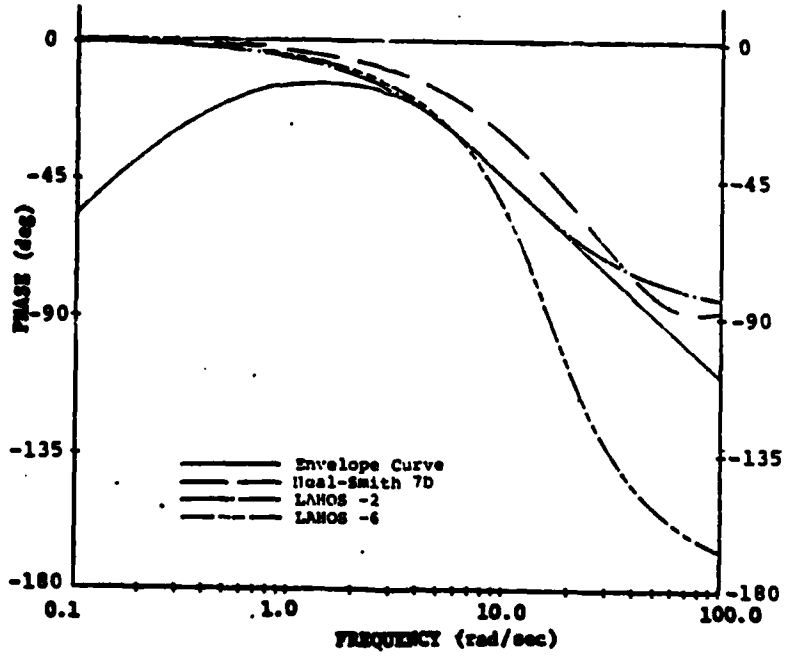

Figure B-4 Lower Phase Envelope and Critical Added Dynamics

APPENDIX C
MISMATCH WEIGHTING

The previously developed envelopes of Maximum Unnoticeable Added Dynamics (MUAD) emphasized the desirability and importance of a K or K/S response in the crossover region. The envelopes can not only be used to check match quality between a high order system and its low order equivalent, but also to try to ensure a high quality match. Two possible methods of doing this are:

1) Penalize the match by adding a large mismatch constant whenever added dynamics or the mismatch between a high and a low order system fall outside the envelope; or
2) Apply a mismatch weighting factor which is an inverse function of the allowable gain or phase mismatch (from the envelopes) at any frequency.

The penalty method suffered from two major faults that would be complicated to correct. The first fault was equal penalties for any amount of the frequency response outside the envelope (e.g., equal penalties whether the frequency response was 1 dB or 10 dB beyond the gain envelope) as shown in Figure C-1a. This is easily corrected by making the mismatch penalty proportional to the amount of the frequency response outside the envelope.

Even if the first fault is corrected, equal amounts of frequency response outside the envelope will be penalized equally, independent of frequency (e.g., a 1 dB gain excess beyond the envelope at low or high frequencies receives the same penalty as a 1 dB excess in the more important crossover region), as shown in Figure C-1b. This fault could be corrected by a frequency dependent weighting factor, but this would be similar to the second method. Due to the complications in correcting these faults, it would be simpler to use the mismatch weighting factors in the first place.

The mismatch weighting factors were developed based on the definition of mismatch from Figure 1 and the unnoticeable gain and phase additions defined by the envelopes of Maximum Unnoticeable Added Dynamics. Since the envelope curves are the maximum additions unnoticeable to pilots, and therefore their mismatches are also the maximum unnoticeable, the weighting factors were defined so as to equate this maximum mismatch. Calculation of the weighting factors is illustrated in Figure C-2 for an arbitrary gain response. Assigning a weighting factor of 1.0 to the largest individual mismatch resulted in weighting factors that increased other mismatches to this value.

For each envelope there were two sets of weighting factors, one each for the upper and lower curves, due to asymmetric envelope curves. Figure C-3 contains the weighting factors for the CTOL envelopes of Maximum Unnoticeable Added Dynamics.

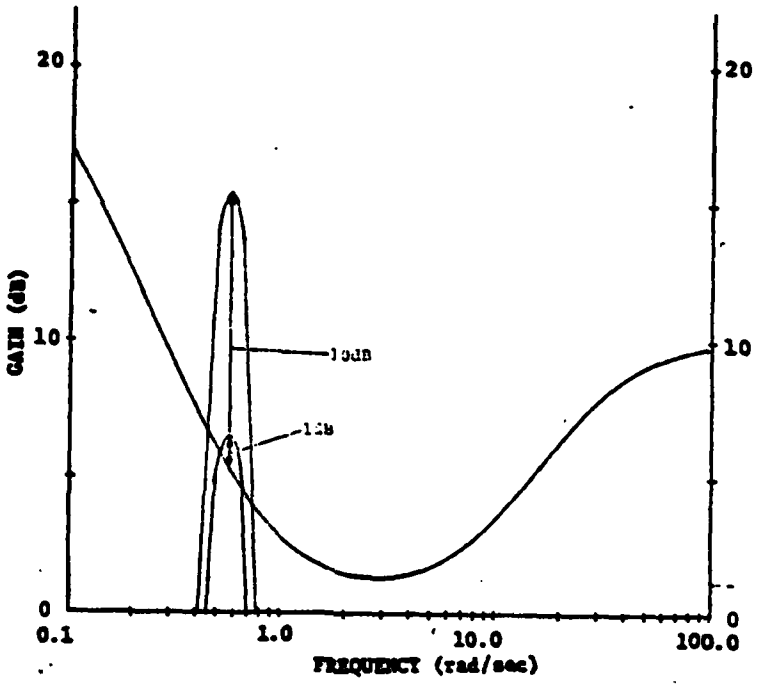

Figure C-1a Two Problems with the Penalty Method for Mismatch weighting

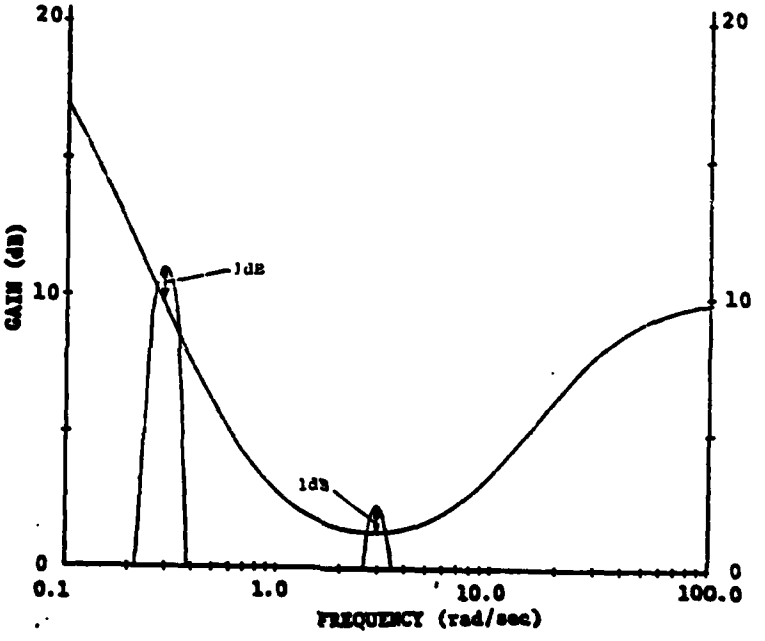

Figure C-1b Two Problems with the Penalty Method for Mismatch Weighting

$$\text{Weighting Factor}_i = WF_i \qquad \text{Weighting Factor}_{G_{max}} = 1.0$$

$$1.0(G_{max})^2 = WF_1(G_1)^2 = \ldots\ldots = WF_i(G_i)^2 = \ldots = WF_n(G_n)^2$$

$$WF_i = \frac{(G_{max})^2}{(G_i)^2}$$

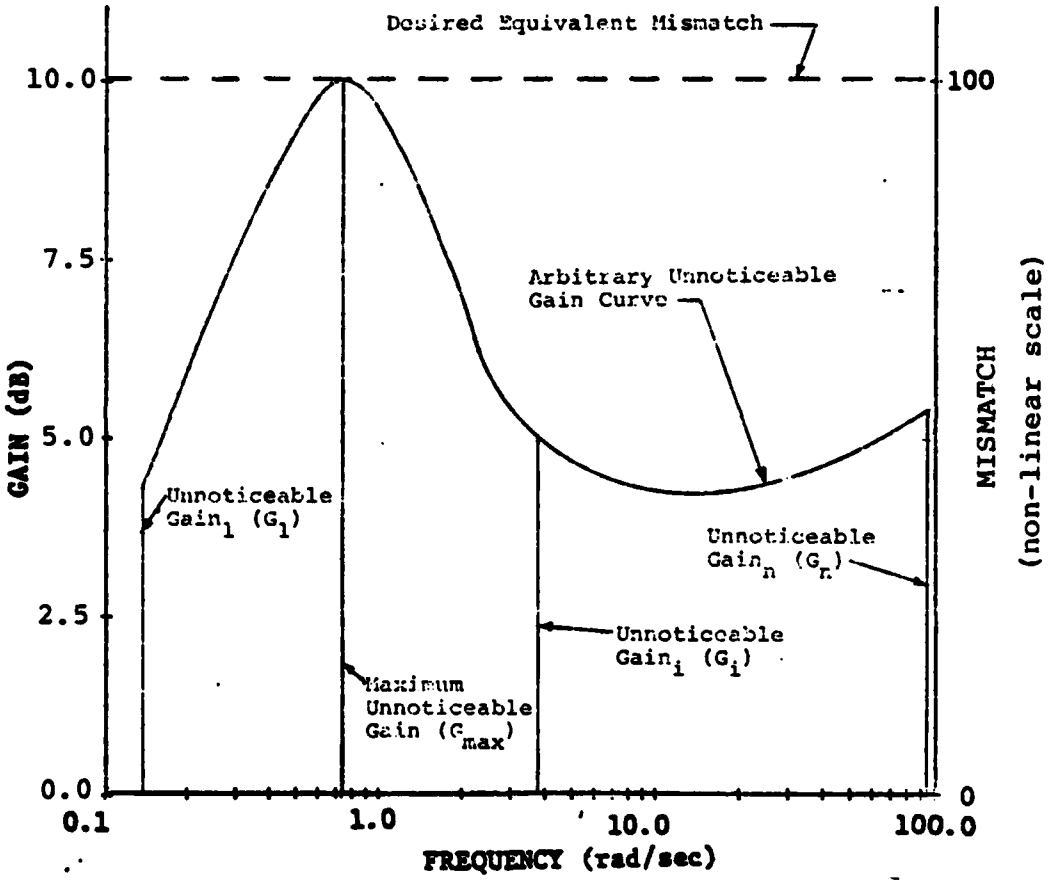

Figure C-2 Calculation of Weighting Factors for an Arbitrary Unnoticeable Gain Curve

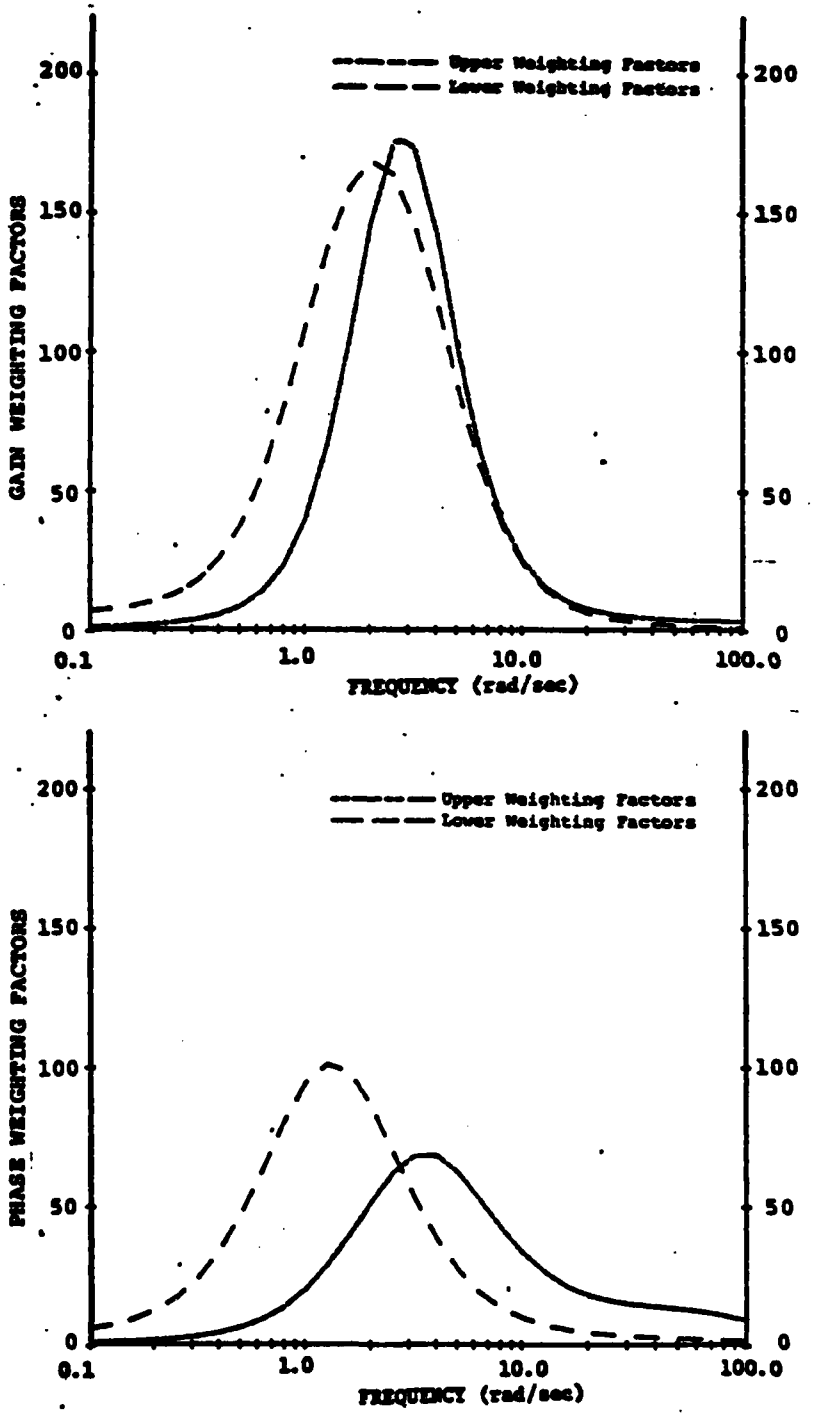

Figure C-3 CTOL Gain and Phase Weighting Factors

APPENDIX D

LAHOS AND NEAL-SMITH EQUIVALENT SYSTEMS

This appendix contains four tables of equivalent systems for the Neal-Smith and LAHOS configurations. The equivalent systems were obtained by matching the high order pitch rate transfer functions of the various configurations to low order equivalent transfer functions of the form:

$$\frac{\dot{\theta}}{F_S} = \frac{K_{\dot{\theta}}\left(\frac{S}{L_{\alpha_e}} + 1\right)e^{-\tau S}}{\frac{S^2}{\omega_{SP_e}^2} + 2\frac{\zeta_{SP_e}}{\omega_{SP_e}}S + 1}.$$

The equivalent systems were calculated using the most recent version of the matching program, both with and without the weighting factors described previously. Tables D-1 and D-2 contain the LAHOS equivalents (D-1: Standard Weighting; D-2: Weighting Factors), and Tables D-3 and D-4 the Neal-Smith equivalents (D-3: Standard Weighting; D-4: Weighting Factors).

Table D-1. LAHOS Equivalent Systems - Standard Weighting

Configuration Number	L_{η_q} Fixed at Basic Airplane Value												L_{η_q} a Free Search Parameter										Pilot Rating	
	τ (sec)	Level*	ω_{sp} (rad sec^{-1})	Level*	ζ_{SP}	Level*	L_{η_q}	n/α (g rad^{-1})	F_g/n (lb g^{-1})	Level*	Level* $F_g/n/\omega_{sp}$ vs ζ_{sp}	Cost	τ (sec)	Level*	ω_{sp} (rad sec^{-1})	Level*	ζ_{sp}	Level*	L_{η_q}	n/α (g rad^{-1})	Cost	Overall	Approach
1-A	0.038	1	1.504	1	1.179	1	0.714	4.5	10.5	1	1-2	25.0	0.028	1	0.868	3	1.769	2	0.214	1.4	20.0	6	6
B	0.026	1	1.309	1	1.040	1			10.5	1		22.4	0.026	1	0.820	3	1.418	2	0.259	1.6	17.9	5	–
C	0.035	1	1.128	1	0.883	1			7.4	1		11.1	0.037	1	0.855	2	1.040	1	0.381	2.4	8.46	4, 4	–, –
1	0.088	1	1.005	1	0.747	1			7.7	1		0.084	0.088	1	0.987	1	0.753	1	0.884	4.4	0.048	4, 4	–, 2
2	0.147	2	0.856	1	0.887	1			6.8	1		5.90	0.142	2	1.154	1	0.652	1	1.132	7.2	4.12	5	–
3	0.167	2	0.844	2-3	0.575	1			10.1	1		56.8	0.143	2	1.746	4	0.710	1	6.393	40.7	11.3	9, 10	6, 6
4	0.228	3	0.720	2-3	0.488	1			6.8	1		154.0	0.127	2	1.479	4	0.688	1	11.986	76.3	6.08	10	–
6	0.161	2	1.003	1	0.744	1			6.8	1		0.308	0.161	2	0.997	1	0.746	1	0.703	4.5	0.306	5, –	2, 5
8	0.234	3	0.974	1	0.702	1			12.7	1		13.1	0.230	3	1.154	1	0.666	1	1.076	6.9	11.8	8	5
11	0.238	3	1.007	1	0.750	1			14.8	1		0.335	0.239	3	0.981	1	0.759	1	0.672	4.3	0.302	8	5
2-A	0.034	1	3.477	1	0.648	1			38.9	2		17.9	0.043	1	3.338	1	0.782	1	0.533	3.4	7.66	4, 6	2, 3
C	0.043	1	2.887	1	0.638	1			28.4	2		5.65	0.047	1	2.595	1	0.703	1	0.608	3.9	3.41	4, 1.5, 1.5, 3	–, –, –, 3
1	0.088	1	2.317	1	0.575	1			31.7	2		0.040	0.069	1	2.311	1	0.579	1	0.706	4.5	0.029	2, 2, –	–, –, 3
2	0.143	2	2.160	1	0.535	1			29.3	2		4.12	0.140	2	2.226	1	0.500	1	0.804	5.1	3.14	4, 4.5	2, 2
3	0.186	2	1.835	1	0.497	1			21.9	1		34.6	0.174	2	2.108	1	0.378	1	1.181	7.5	21.4	6	–
4	0.210	3	1.500	1	0.494	1			18.0	1		84.5	0.173	2	2.241	1	0.318	2	2.866	18.2	31.3	9, –, –	–, 5, 3
6	0.161	2	2.309	1	0.570	1			25.7	1		0.301	0.161	2	2.311	1	0.569	1	0.718	4.6	0.301	5	1.5
7	0.193	2	2.281	1	0.558	1			27.7	1		2.15	0.192	2	2.302	1	0.546	1	0.741	4.7	2.04	7, 6	4, 3
8	0.284	4	1.999	1	0.459	1			36.2	2		84.0	0.274	4	2.247	1	0.361	1	1.123	7.1	51.4	10	5
10	0.332	4	1.713	1	0.391	1			36.2	2		193.0	0.261	4	2.714	1	0.221	3	5.449	34.7	109.0	10	6
11	0.239	3	2.326	1	0.577	1			27.7	1		0.280	0.239	3	2.318	1	0.581	1	0.705	4.5	0.287	8	4
3-C	0.030	1	2.376	1	0.274	2			39.2	2		17.4	0.035	1	2.315	1	0.305	2	0.589	3.7	10.6	2, 5	–, 5
0	0.087	1	2.104	1	0.141	4			38.2	2		0.097	0.068	1	2.102	1	0.142	4	0.706	4.5	0.089	4, 5	–, –
1	0.088	1	2.208	1	0.251	2			43.5	3		0.077	0.068	1	2.204	1	0.253	2	0.706	4.5	0.056	4, 7, 5	–, –, 5
2	0.148	2	2.133	1	0.239	3			33.1	2		7.02	0.145	2	2.169	1	0.224	3	0.797	5.1	5.14	7, –	–, 6
3	0.202	3	1.945	1	0.231	3			33.1	2		70.7	0.187	2	2.115	1	0.172	3	1.173	7.6	40.3	10, –	–, 7
6	0.161	2	2.206	1	0.250	2			37.1	2		0.305	0.161	2	2.204	1	0.251	2	0.712	4.5	0.303	7, 6	5, 5
7	0.194	2	2.195	1	0.247	3			26.3	1		2.27	0.193	2	2.201	1	0.244	3	0.728	4.6	2.20	8	5
4-C	0.057	1	2.584	1	1.297	1			16.9	1		0.868	0.060	1	2.434	1	1.417	2	0.605	3.9	0.524	3, 3	1.5, 2
0	0.089	1	2.130	1	1.247	1			9.2	1		0.013	0.070	1	2.113	1	1.259	1	0.700	4.5	0.010	6	–
1	0.089	1	2.024	1	1.073	1			13.9	1		0.019	0.089	1	2.007	1	1.084	1	0.699	4.5	0.014	2	–
3	0.172	2	1.460	1	0.806	1			12.6	1		17.7	0.154	2	2.296	1	0.685	1	2.305	14.7	9.12	5, 8, 7	–, 5, 2
4	0.190	2	1.146	1	0.720	1			15.6	1		39.9	0.135	2	2.582	2-3	0.650	1	7.634	48.6	6.75	7, 6, –	4, 3, 6
6	0.161	2	2.009	1	1.060	1			13.9	1		0.310	0.161	2	2.025	1	1.050	1	0.729	4.6	0.305	4	1.5
7	0.191	2	1.966	1	1.029	1			20.9	1		2.01	0.190	2	2.055	1	0.977	1	0.800	5.1	1.87	3	3
10	0.314	4	1.335	1	0.643	1			27.4	1		144.0	0.161	2	3.016	4	0.454	1	198.38	1,263.0	17.7	9	6
11	0.240	3	2.033	1	1.077	1			13.9	1		0.261	0.240	3	2.017	1	1.087	1	0.701	4.5	0.257	8	3
5-1	0.089	1	3.939	1	0.642	1			37.0	2		0.020	0.089	1	3.936	1	0.645	1	0.710	4.5	0.014	7, 5	–, 4
3	0.174	2	2.950	1	0.540	1			31.0	2		18.2	0.167	2	3.105	1	0.455	1	0.920	5.9	12.6	8, 6, 4.5, –, –	–, 2, 3, 4, 3
4	0.193	2	2.347	1	0.635	1			22.7	1		40.4	0.178	2	2.790	1	0.436	1	1.339	8.5	23.8	6	2
5	0.206	3	1.774	1	0.833	1			18.6	1		61.7	0.142	2	3.580	1	0.413	1	7.165	45.6	9.85	7	2
6	0.160	2	3.908	1	0.534	1			35.1	2		0.283	0.160	2	3.908	1	0.531	1	0.719	4.6	0.277	6	3
7	0.190	2	3.821	1	0.519	1			30.4	2		1.81	0.189	2	3.835	1	0.507	1	0.737	4.7	1.68	6	2
11	0.240	3	3.952	1	0.541	1			27.0	1		0.247	0.240	3	3.961	1	0.542	1	0.712	4.5	0.245	7	3
6-1	0.320	4	1.303	1	0.560	1			21.4	1		170.0	0.163	2	2.770	4	0.413	1	111.26	708.3	23.7	10	–
2	0.083	1	1.739	1	0.838	1	0.714	4.5	18.9	1	1-2	1.12	0.080	1	1.891	1	0.758	1	0.896	5.7	0.120	2	–

*Levels refer to MIL F 8785C, class IV, category C, except Level 4 which is defined as worse than Level 3

Notes
1. Configurations are defined in AFFDL TR 78 122
2. All configurations, frequency range 0.1 - 10 rad/sec

Table D-2. LAHOS Equivalent Systems - Weighting Factors

Configuration Number	L_{α} Fixed at Basic Airplane Value												L_{α} a Free Search Parameter										Pilot Rating	
	τ (sec)	Level*	ω_{np} (rad sec^{-1})	Level*	ζ_{SP}	Level*	L_{α}	n/α (g rad^{-1})	Fg/m (lb g^{-1})	Level*	Level* $F_g/m/\omega_{SS}$ vs ζ_{SP}	Cost	τ (sec)	Level*	ω_{np} (rad sec^{-1})	Level*	ζ_{SP}	Level*	L_{α}	n/α (g rad^{-1})	Fg/m (lb g^{-1})	Cost	Overall	Approach
1-A	0.026	1	1.374	1	1.324	2	0.714	4.5	10.5	1	1-2	41.6	0.021	1	0.610	3	2.281	3	0.128	0.8	28.9	6	6	
B	0.022	1	1.195	1	1.142	1			10.5	1		35.9	0.019	1	0.639	3	1.637	2	0.176	1.1	24.2	5	–	
C	0.030	1	1.068	1	0.927	1			7.4	1		16.6	0.032	1	0.776	2	1.060	1	0.331	2.1	10.7	4, 4	–, –	
1	0.087	1	1.002	1	0.748	1			7.7	1		0.086	0.088	1	0.995	1	0.760	1	0.683	4.3	0.059	4, 4	–, 2	
2	0.148	2	0.980	1	0.686	1			6.8	1		7.02	0.141	2	1.256	1	0.693	1	1.375	8.8	5.74	5	–	
3	0.201	3	0.908	1	0.557	1			10.1	1		67.6	0.135	2	1.813	4	0.839	1	8.095	51.5	17.5	9, 10	6, 6	
4	0.234	3	0.808	2-3	0.440	1			6.8	1		184.0	0.121	2	1.478	4	0.766	1	13.692	87.2	9.80	10	–	
6	0.158	2	1.004	1	0.744	1			6.8	1		0.412	0.158	2	0.996	1	0.745	1	0.700	4.5	0.414	5, –	2, 5	
8	0.231	3	1.002	1	0.706	1			12.7	1		15.0	0.226	3	1.229	1	0.706	1	1.217	7.7	14.1	8	5	
11	0.235	3	1.004	1	0.750	1			14.8	1		0.504	0.235	3	0.980	1	0.753	1	0.671	4.3	0.488	9	5	
2-A	0.024	1	3.277	1	0.855	1			36.9	2		23.6	0.035	1	3.185	1	0.749	1	0.509	3.2	9.37	4, 6	2, 3	
C	0.038	1	2.605	1	0.638	1			28.4	2		7.11	0.042	1	2.539	1	0.680	1	0.602	3.8	4.10	4, 1.5, 1.5, 3	–, –, –, 3	
1	0.088	1	2.312	1	0.574	1			31.7	2		0.049	0.088	1	2.308	1	0.577	1	0.706	4.5	0.039	2, 2, –	–, –, 3	
2	0.144	2	2.209	1	0.536	1			29.3	2		5.10	0.139	2	2.267	1	0.509	1	0.830	5.3	3.82	4, 4.5	2, 2	
3	0.191	2	1.957	1	0.481	1			21.9	1		43.9	0.173	2	2.232	1	0.396	1	1.375	8.8	28.1	8	–	
4	0.218	3	1.660	1	0.473	1			18.0	1		108.0	0.163	2	2.391	1	0.368	1	3.786	24.1	45.0	8, –, –	–, 5, 3	
6	0.158	2	2.309	1	0.569	1			25.7	1		0.400	0.158	2	2.308	1	0.570	1	0.711	4.5	0.407	5	1.5	
7	0.189	2	2.299	1	0.557	1			27.7	1		2.59	0.188	2	2.311	1	0.552	1	0.738	4.7	2.47	7, 6	4, 3	
9	0.288	4	2.147	1	0.463	1			36.2	2		75.3	0.271	4	2.354	1	0.394	1	1.208	7.7	61.3	10	5	
10	0.340	4	1.935	1	0.379	1			36.2	2		231.0	0.215	3	2.875	2-3	0.289	2	11.222	71.4	156.0	10	6	
11	0.235	3	2.315	1	0.575	1			27.7	1		0.436	0.236	3	2.309	1	0.578	1	0.701	4.5	0.421	8	4	
3-C	0.021	1	2.312	1	0.274	2			39.2	2		20.4	0.026	1	2.279	1	0.290	2	0.586	3.7	12.7	2, 5	–, 5	
0	0.067	1	2.102	1	0.141	4			38.2	2		0.112	0.067	1	2.101	1	0.141	4	0.707	4.5	0.086	4, 5	–, –	
1	0.087	1	2.204	1	0.251	2			43.5	3		0.091	0.087	1	2.203	1	0.252	2	0.707	4.5	0.089	4, 7, 5	–, –, 5	
2	0.150	2	2.188	1	0.238	3			33.1	2		8.15	0.145	2	2.191	1	0.230	3	0.812	5.2	6.01	7, –	–, 6	
3	0.209	3	2.055	1	0.220	3			33.1	2		85.2	0.186	2	2.183	1	0.186	3	1.331	8.5	52.4	10, –	–, 7	
6	0.158	2	2.204	1	0.250	2			37.1	2		0.419	0.158	2	2.202	1	0.251	2	0.707	4.5	0.415	7, 6	5, 5	
7	0.190	2	2.202	1	0.246	3			26.3	1		2.61	0.190	2	2.203	1	0.246	3	0.719	4.6	2.58	8	5	
4-C	0.055	1	2.532	1	1.298	1			16.9	1		1.19	0.057	1	2.379	1	1.405	2	0.592	3.8	0.624	3, 3	1.5, 2	
0	0.089	1	2.125	1	1.246	1			9.2	1		0.017	0.089	1	2.103	1	1.259	1	0.686	4.4	0.012	6	–	
1	0.088	1	2.019	1	1.072	1			13.9	1		0.026	0.089	1	2.002	1	1.081	1	0.688	4.4	0.018	2	–	
3	0.175	2	1.545	1	0.809	1			12.6	1		22.4	0.146	2	2.644	1	0.625	1	3.415	21.7	13.4	5, 8, 7	–, 5, 2	
4	0.194	2	1.237	1	0.711	1			15.6	1		49.7	0.129	2	2.654	2-3	0.719	1	9.015	57.4	9.91	7, 6, –	4, 3, 5	
6	0.158	2	2.013	1	1.058	1			13.9	1		0.419	0.158	2	2.025	1	1.052	1	0.726	4.6	0.411	4	5	
7	0.187	2	1.991	1	1.030	1			20.9	1		2.54	0.186	2	2.092	1	0.981	1	0.821	5.2	2.35	3	3	
10	0.321	4	1.530	1	0.836	1			27.4	1		177.0	0.165	2	3.032	4	0.509	1	104.35	664.3	24.1	9	6	
11	0.236	3	2.026	1	1.072	1			13.9	1		0.394	0.237	3	2.006	1	1.082	1	0.686	4.4	0.396	6	3	
5-1	0.088	1	3.931	1	0.541	1			37.0	2		0.024	0.089	1	3.930	1	0.543	1	0.710	4.5	0.018	7, 5	–, 4	
3	0.178	2	3.109	1	0.542	1			31.0	2		23.2	0.166	2	3.216	1	0.470	1	0.981	6.2	15.7	8, 6, 4.5, –, –	–, 2, 3, 4, 3	
4	0.200	2	2.559	1	0.632	1			22.7	1		52.9	0.175	2	2.986	1	0.446	1	1.611	10.3	31.7	6	2	
5	0.213	3	2.003	1	0.827	1			18.6	1		82.0	0.133	2	3.657	1	0.448	1	8.348	53.1	14.3	7	2	
6	0.158	2	3.905	1	0.534	1			35.1	2		0.382	0.158	2	3.905	1	0.534	1	0.714	4.5	0.382	6	3	
7	0.186	2	3.845	1	0.521	1			30.4	2		2.26	0.185	2	3.849	1	0.516	1	0.734	4.7	2.13	6	2	
11	0.236	3	3.935	1	0.540	1			27.0	1		0.378	0.236	3	3.934	1	0.542	1	0.707	4.5	0.381	7	3	
6-1	0.328	4	1.507	1	0.530	1			21.4	1		216.0	0.167	2	2.756	4	0.471	1	68.142	433.8	33.6	10	–	
2	0.083	1	1.760	1	0.815	1	0.714	4.5	18.9	1	1-2	1.88	0.079	1	1.883	1	0.757	1	0.890	5.7	0.161	2	–	

*Levels refer to MIL F-8785C, class IV, category C, except Level 4 which is defined as worse than Level 3

Notes:
1. Configurations are defined in AFFDL-TR-78-122
2. All configurations, frequency range 0.1 - 10 rad/sec

Table D-3. Neal-Smith Equivalent Systems - Standard Weighting

Configuration Number	L_{α_q} Fixed at Basic Airplane Value												L_{α_q} a Free Search Parameter								Pilot Rating	
	τ (sec)	Level*	$\omega_{n_{SP}}$ (rad sec^{-1})	Level*	ζ_{SP}	Level*	L_{α_q}	n/α (g rad^{-1})	Fg/n (lb g^{-1})	Level*	Level* Fg/n_{SS} vs ζ_{SP}	Cost	τ (sec)	Level*	$\omega_{n_{SP}}$ (rad sec^{-1})	Level*	ζ_{SP}	Level*	L_{α_q}	n/α (g rad^{-1})	Cost	Pilot M	Pilot W
1A	–	1	3.140	1	0.389	1	1.241	18.5	7.2	1	1-2	122.0	0.020	1	2.536	1	0.654	1	0.429	6.4	0.860	6, 4	5
B	0.009	1	3.086	1	0.684	1			6.3	1		4.97	0.017	1	2.810	1	0.832	1	0.890	13.3	0.766	3.5	3
C	0.079	1	3.024	1	0.675	1			8.1	1		3.72	0.085	1	2.778	1	0.789	1	0.929	13.8	0.667	3.5, 5	4
D	0.018	1	2.190	2-3	0.692	1			6.0	1		0.009	0.018	1	2.216	2-3	0.687	1	1.269	18.9	0.009	4.5, 5	3, 4
E	0.129	2	1.763	2-3	0.582	1			9.0	1		21.9	0.104	2	2.532	4	0.483	1	3.516	52.4	7.21	6	–
F	0.161	2	1.372	4	0.551	1			10.2	1		74.0	0.074	1	2.480	4	0.571	1	13.714	204.4	2.31	8	8
G	0.186	2	0.779	4	0.743	1			5.3	1		151.0	0.043	1	1.552	4	1.089	1	175.75	2,619.9	13.1	8.5	8.5
2A	–	1	5.958	1	0.462	1			5.5	1		17.3	0.008	1	5.890	1	0.551	1	0.921	13.7	2.19	4.5	4
B	0.058	1	5.689	1	0.420	1			5.9	1		12.9	0.073	1	5.669	1	0.529	1	0.940	14.0	1.51	6, 6	4, 5
C	0.003	1	6.131	1	0.648	1			4.6	1		1.06	0.008	1	6.183	1	0.703	1	1.145	17.1	0.431	3	–
D	0.018	1	4.898	1	0.702	1			6.5	1		0.006	0.019	1	4.915	1	0.704	1	1.243	18.5	0.008	2.5, 3	2.5
E	0.080	1	4.406	1	0.680	1			3.8	1		0.912	0.077	1	4.458	1	0.639	1	1.342	20.0	0.564	4	– (7, 8)
F	0.107	2	3.579	1	0.681	1			5.5	1		5.64	0.099	1	3.808	1	0.575	1	1.606	23.9	3.20	3	– (7)
G	0.176	2	3.499	1	0.867	1			5.5	1		9.49	0.167	2	3.784	1	0.523	1	1.707	25.4	5.87	7	–
H	0.126	2	2.550	1	0.801	1			6.3	1		16.2	0.098	1	3.796	2-3	0.521	1	4.083	60.9	4.62	5, 6	5.5
I	0.196	2	2.512	1	0.785	1			4.8	1		21.3	0.159	2	4.030	2-3	0.488	1	5.533	82.5	6.66	8	8
J	0.139	2	1.387	4	1.380	2			5.2	1		25.7	0.136	2	0.963	4	1.477	2	0.668	9.8	20.8	6	6
3A	0.020	1	9.809	2	0.639	1			8.4	1		0.009	0.020	1	9.835	2	0.638	1	1.244	18.5	0.008	4, 5	4, 4 (7)
B	0.073	1	8.555	2	0.702	1			4.3	1		0.194	0.070	1	8.423	2	0.676	1	1.277	19.0	0.106	4.5	–
C	0.093	1	6.916	1	0.888	1			6.2	1		0.893	0.088	1	6.791	1	0.815	1	1.336	19.9	0.539	4	3
D	0.106	2	5.008	1	1.337	2			5.3	1		2.03	0.097	1	5.240	1	1.069	1	1.647	24.8	1.18	4	4
E	0.116	2	2.741	1	2.727	3			4.7	1		3.06	0.109	2	2.358	1	2.671	3	1.082	15.8	2.25	4	4
4A	0.018	1	4.998	1	0.281	2			7.0	1		0.009	0.018	1	5.005	1	0.280	2	1.247	18.8	0.005	5.5	5
B	0.090	1	4.792	1	0.291	2			5.6	1		3.03	0.086	1	4.825	1	0.270	2	1.380	20.3	1.77	–	7
C	0.133	2	4.320	1	0.350	1			3.9	1	1-2	24.3	0.119	2	4.507	1	0.263	2	1.746	28.0	11.8	8.5	–
D	0.189	2	3.473	1	0.586	1			4.9	1	1-2	80.2	0.111	2	4.610	2-3	0.233	3	5.251	78.3	13.6	8, 9	–
E	0.197	2	2.048	2-3	1.513	2			3.9	1	1-2	152.0	0.196	2	1.144	2-3	2.163	3	0.457	6.8	131.0	7.5	–
5A	0.018	1	5.100	1	0.181	3			7.3	1	3	0.009	0.018	1	5.098	1	0.181	3	1.245	18.6	0.008	7	5, 6
B	0.093	1	4.958	1	0.190	3			7.1	1	3	4.19	0.088	1	4.984	1	0.176	3	1.387	20.4	2.39	–	7
C	0.140	2	4.607	1	0.244	3			7.3	1	1-2	36.7	0.124	2	4.764	1	0.175	3	1.807	28.9	18.6	9	7
D	0.182	2	3.861	1	0.484	1			7.9	1	1-2	130.0	0.113	2	4.856	1	0.154	3	5.802	83.5	17.5	8.5, 9	8
E	0.215	3	2.372	1	1.539	2	1.241	18.5	5.4	1	1-2	264.0	0.066	1	4.963	4	0.422	1	313.23	4,699.3	172.0	8	8
6A	–	1	4.661	1	0.339	2	2.385	50.0	6.2	1	1-2	125.0	0.020	1	3.736	1	0.647	1	0.739	15.5	0.249	5	6
B	0.004	1	4.470	1	0.841	1			4.5	1		3.21	0.014	1	4.060	1	0.790	1	1.848	34.5	0.364	1, 2.5	4 (5, 7)
C	0.018	1	3.398	2-3	0.676	1			6.0	1		0.009	0.018	1	3.400	2-3	0.671	1	2.381	49.9	0.007	4	6 (8, 7)
D	0.101	2	2.943	2-3	0.819	1			4.9	1		4.86	0.084	1	3.608	4	0.542	1	4.585	86.7	1.24	5.5	– (8)
E	0.132	2	2.330	4	0.807	1			5.6	1		22.8	0.065	1	3.606	4	0.593	1	18.476	346.4	0.431	8.5	7
F	0.158	2	1.325	4	0.847	1			5.0	1		61.6	0.050	1	2.265	4	1.126	1	161.27	3,380.7	10.7	8	8.5, 10
7A	–	1	8.235	1	0.443	1			4.9	1		6.17	0.006	1	8.328	1	0.585	1	1.862	38.8	0.428	4, 5	2
B	0.004	1	8.558	1	0.661	1			3.1	2-3		0.181	0.009	1	8.770	1	0.709	1	2.257	47.3	0.06	3	–
C	0.018	1	7.293	1	0.735	1			4.4	1		0.005	0.020	1	7.379	1	0.744	1	2.374	49.8	0.008	3, 3	1.5, 4
D	0.082	1	6.789	1	0.730	1			3.0	2-3		0.09	0.059	1	6.783	1	0.688	1	2.600	52.4	0.04	5.5	–
E	0.083	1	5.730	1	0.749	1			4.3	1		0.748	0.077	1	5.871	1	0.661	1	2.826	59.2	0.313	6	5
F	0.100	1	4.233	1	0.873	1			4.7	1		2.65	0.079	1	5.618	2-3	0.630	1	6.008	125.9	0.512	3, 4, 4	7, 7, 7 (7, 8)
G	0.108	2	3.439	2-3	1.021	1			4.9	1		3.91	0.075	1	6.854	4	0.872	1	15.851	332.3	1.38	5	6
H	0.112	2	2.266	4	1.482	2			4.7	1		5.61	0.108	2	1.720	4	1.439	2	1.528	32.0	3.54	–	5
8A	0.018	1	16.465	2	0.680	1			5.2	1		0.009	0.018	1	16.481	2	0.682	1	2.387	50.0	0.008	5	4
B	0.051	1	13.476	2	0.732	1			3.3	2-3		0.495	0.049	1	13.367	1	0.614	1	2.499	52.4	0.306	3.5	– (7)
C	0.059	1	10.320	1	0.872	1			4.8	1		1.76	0.057	1	10.415	1	0.781	1	2.882	56.4	1.10	3.5	3
D	0.076	1	9.151	1	1.531	2			5.1	1		0.084	0.070	1	8.812	1	1.318	2	2.705	56.7	0.039	2	4
E	0.082	1	4.980	1	3.171	3	2.385	50.0	4.6	1	1-2	0.130	0.077	1	4.427	1	2.908	3	2.288	47.9	0.081	2.5, 3	5

*Levels refer to MIL-F-8785C, class IV, category A, except Level 4 which is defined as worse than Level 3

Notes:
1. Configurations are defined in AFFDL-TR-70-74
2. Configurations 8A - 8E, frequency range 0.1 - 20 rad/sec
3. All others, 0.1 - 10 rad/sec
4. Pilot Ratings in parentheses are from AFFDL-TR-74-8

Table D-4. Neal-Smith Equivalent Systems - Weighting Factors

Configuration Number	L_α Fixed at Basic Airplane Value												L_α a Free Search Parameter									Pilot Rating	
	T (sec)	Level*	ω_{sp} (rad sec^{-1})	Level*	ζ_{sp}	Level*	L_α	a/n (g rad^{-1})	F_s/n (lb g^{-1})	Level*	Level* F_s/n_{ss} vs ζ_{sp}	Cost	T (sec)	Level*	ω_{sp} (rad sec^{-1})	Level*	ζ_{sp}	Level*	L_α	a/n (g rad^{-1})	Cost	Pilot M	Pilot W
1A	–	1	2.986	1	0.473	1	1.241	18.5	7.2	1	1-2	168.0	0.019	1	2.506	1	0.881	1	0.413	6.2	1.09	6, 4	5
B	0.006	1	3.011	1	0.712	1			6.3	1		6.93	0.015	1	2.765	1	0.825	1	0.867	12.9	0.982	3.5	3
C	0.074	1	2.958	1	0.885	1			6.1	1		5.50	0.082	1	2.733	1	0.794	1	0.893	13.3	0.832	3.5, 5	4
D	0.018	1	2.196	2-3	0.882	1			6.0	1		0.001	0.018	1	2.198	2-3	0.881	1	1.246	18.6	0.0003	4.5, 5	3, 4
E	0.133	2	1.885	2-3	0.582	1			9.0	1		27.6	0.101	2	2.564	4	0.519	1	3.619	53.9	9.75	6	–
F	0.188	2	1.514	4	0.533	1			10.2	1		94.2	0.073	1	2.466	4	0.800	1	13.984	203.7	3.44	8	8
G	0.191	2	0.901	4	0.678	1			5.3	1		187.0	0.054	1	1.648	4	0.981	1	70.486	1,050.9	22.1	8.5	8.5
2A	–	1	5.820	1	0.445	1			5.5	1		20.4	0.003	1	5.738	1	0.532	1	0.902	13.4	2.92	4.5	4
B	0.048	1	5.440	1	0.426	1			5.9	1		18.9	0.068	1	5.561	1	0.522	1	0.912	13.6	2.16	5, 6	4, 5
C	–	1	6.013	1	0.639	1			4.6	1		1.22	0.005	1	6.075	1	0.682	1	1.149	17.1	0.529	3	–
D	0.018	1	4.904	1	0.704	1			6.5	1		0.005	0.018	1	4.903	1	0.700	1	1.251	18.6	0.0002	2.5, 3	2.5
E	0.080	1	4.667	1	0.686	1			3.8	1		1.19	0.076	1	4.485	1	0.652	1	1.338	19.9	0.763	4	– (7,8)
F	0.108	2	3.706	1	0.891	1			5.5	1		7.23	0.097	1	3.855	1	0.801	1	1.804	23.9	4.17	3	– (7)
G	0.175	2	3.836	1	0.676	1			5.5	1		12.0	0.163	2	3.821	1	0.575	1	1.688	25.2	7.06	7	–
H	0.130	2	2.722	1	0.814	1			6.3	1		18.7	0.096	1	3.808	2-3	0.553	1	4.050	60.4	6.48	5, 6	5.5
I	0.188	2	2.686	1	0.796	1			4.8	1		27.2	0.156	2	3.985	2-3	0.524	1	5.157	76.9	9.46	8	8
J	0.143	2	1.498	4	1.384	2			5.2	1		33.1	0.138	2	0.917	4	1.899	2	0.582	8.7	28.7	6	6
3A	0.019	1	9.782	2	0.635	1			8.4	1		0.01	0.018	1	9.726	2	0.631	1	1.249	18.6	0.0002	4, 5	4,4 (7)
B	0.073	1	8.698	2	0.710	1			4.3	1		0.291	0.070	1	8.540	2	0.690	1	1.272	19.0	0.170	4.5	–
C	0.093	1	7.149	1	0.912	1			6.2	1		1.29	0.087	1	6.945	1	0.849	1	1.326	19.8	0.821	4	3
D	0.107	2	5.297	1	1.398	2			6.3	1		2.88	0.097	1	5.365	1	1.133	1	1.620	24.1	1.71	4	4
E	0.116	2	2.973	1	2.911	3			4.7	1		4.32	0.109	2	2.434	1	2.880	3	1.043	15.5	3.23	4	4
4A	0.018	1	5.001	1	0.281	2			7.0	1		0.013	0.018	1	5.001	1	0.280	2	1.249	18.6	0.0001	5, 5	5
B	0.080	1	4.852	1	0.292	2			5.6	1	1-2	3.56	0.085	1	4.851	1	0.278	2	1.364	20.2	2.22	–	7
C	0.138	2	4.512	1	0.349	2			3.9	1	3	29.5	0.117	2	4.566	1	0.285	2	1.739	25.9	15.1	8.5	–
D	0.181	2	3.913	1	0.569	1			4.9	1	1-2	108.0	0.106	2	4.616	2-3	0.266	2	5.217	77.8	19.1	8, 9	–
E	0.208	3	2.733	1	1.571	2			3.9	1	1-2	209.0	0.082	1	5.196	4	0.459	1	132.21	1,970.8	249.0	7.5	–
5A	0.018	1	5.101	1	0.181	3			7.3	1	3	0.015	0.018	1	5.101	1	0.180	3	1.250	18.6	0.0001	7	5, 6
B	0.093	1	5.007	1	0.191	3			7.1	1	3	4.70	0.087	1	5.004	1	0.182	3	1.380	20.3	2.93	–	7
C	0.145	2	4.786	1	0.239	3			7.3	1	1-2	43.1	0.122	2	4.813	1	0.191	3	1.800	26.8	20.9	9	7
D	0.196	2	4.377	1	0.443	1			7.9	1	1-2	172.0	0.107	2	4.853	1	0.170	3	5.572	83.1	24.8	8.5, 9	9
E	0.230	3	3.515	1	1.567	2	1.241	18.5	6.4	1	1-2	357.0	0.082	1	5.208	4	0.278	2	96.706	1,441.6	289.0	8	8
6A	–	1	4.401	1	0.384	1	2.385	50.0	6.2	1	1-2	169.0	0.019	1	3.709	1	0.643	1	0.730	15.3	0.328	6	6
B	–	1	4.351	1	0.638	1			4.5	1		4.00	0.012	1	4.037	1	0.770	1	1.884	34.9	0.447	1, 2.5	4 (5,7)
C	0.018	1	3.395	2-3	0.672	1			6.0	1		0.0004	0.018	1	3.404	2-3	0.670	1	2.405	50.4	0.0003	4	5 (8,7)
D	0.103	2	3.028	2-3	0.623	1			4.9	1		6.11	0.083	1	3.543	4	0.569	1	4.256	80.2	1.72	5.5	– (8)
E	0.137	2	2.478	4	0.609	1			5.6	1		29.3	0.087	1	3.564	4	0.598	1	14.860	311.3	0.866	8.5	7
F	0.164	2	1.480	4	0.863	1			5.0	1		79.3	0.062	1	2.424	4	1.089	1	74.196	1,555.4	17.8	8	8.5, 10
7A	–	1	8.149	1	0.436	1			4.9	1		7.85	0.003	1	8.169	1	0.546	1	1.859	39.0	0.589	4, 5	2
B	0.001	1	8.418	1	0.653	1			3.1	2-3		0.209	0.007	1	8.684	1	0.696	1	2.274	47.7	0.085	3	–
C	0.019	1	7.319	1	0.735	1			4.4	1		0.002	0.018	1	7.297	1	0.729	1	2.401	50.3	0.0003	3, 3	1.5, 4
D	0.082	1	6.837	1	0.734	1			3.0	2-3		0.137	0.059	1	6.803	1	0.709	1	2.478	51.9	0.068	5.5	–
E	0.083	1	5.828	1	0.759	1			4.3	1		1.02	0.076	1	5.876	1	0.686	1	2.744	57.5	0.479	6	5
F	0.100	1	4.367	1	0.890	1			4.7	1		3.53	0.080	1	5.444	2-3	0.884	1	5.278	110.6	0.811	3, 4, 4	7, 7, 7, (7, 8)
G	0.108	2	3.578	2-3	1.045	1			4.9	1		5.20	0.072	1	7.294	4	0.868	1	21.648	453.8	1.91	5	6
H	0.112	2	2.386	4	1.521	2			4.7	1		7.42	0.104	2	1.765	4	1.506	2	1.553	32.6	4.56	–	5
8A	0.019	1	16.649	2	0.606	1			5.2	1		0.008	0.018	1	16.482	2	0.697	1	2.389	50.3	0.001	5	4
B	0.051	1	13.900	2	0.756	1			3.3	2-3		0.832	0.049	1	13.635	2	0.727	1	2.451	51.4	0.575	3.5	–(7)
C	0.080	1	10.886	1	0.925	1			4.8	1		2.87	0.057	1	10.668	1	0.955	1	2.551	53.5	2.01	3.5	3
D	0.077	1	9.536	1	1.588	2			5.1	1		0.130	0.072	1	9.020	1	1.391	2	2.820	54.9	0.068	2	4
E	0.082	1	5.190	1	3.296	3	2.385	50.0	4.6	1	1-2	0.195	0.077	1	4.608	1	3.016	3	2.308	48.4	0.126	2.5, 3	5

GP80-1650-604

*Levels refer to MIL F 8785C, class IV, category A, except Level 4 which is defined as worse than Level 3

Notes

1. Configurations are defined in AFFDL TH 70 74
2. Configurations 8A 8C, frequency range 0.1 20 rad/sec
3. All others, 0.1 10 rad/sec
4. Pilot Ratings in parentheses are from AFFDL-TR-74-8